Subspace Approach to Multidimensional Fault Identification and Reconstruction

Ricardo Dunia and S. Joe Qin
Dept. of Chemical Engineering, University of Texas at Austin, Austin, TX 78712

Fault detection and process monitoring using principal-component analysis (PCA) and partial least squares were studied intensively and applied to industrial processes. The fundamental issues of detectability, reconstructability, and isolatability for multidimensional faults are studied. PCA is used to define an orthogonal partition of the measurement space into two orthogonal subspaces, a principal-component subspace, and a residual subspace. Each multidimensional fault is also described by a subspace on which the fault displacement occurs. Fault reconstruction leads to fault identification and consists of finding a new vector in the fault subspace with minimum distance to the principal-component subspace. The unreconstructed variance is proposed to measure the reliability of the reconstruction procedure and determine the PCA model for best reconstruction. Based on the fault subspace, fault magnitude, and the squared prediction error, necessary and sufficient conditions are provided to determine if the faults are detectable, reconstructable, and isolatable.

Introduction

Process equipment deteriorates with time and use, and requires frequent maintenance. In some processes, equipment degradation affects the quality and yield. However, in other cases, the plant production is not affected by the equipment degradation until a major failure occurs. This type of drastic failure of process equipment is usually very costly because the production would be interrupted for a period of time, and other equipment or product stocks could be affected by such a failure. For this reason, in general, it is important to detect sensor faults as well as process faults that indicate significant deterioration of equipment.

Process disturbances are another source of operational problems in a plant (Ku et al., 1995). Because not all the variables that affect the process are under the control of the plant operations, the changes in one of these variables may take the process operation out of its optimum. Moreover, severe process interaction increases the possibility that a control action, which tends to correct a disturbance in a particular process unit, will affect other units of the plant. This interaction also shows the necessity of monitoring the process in an integrated manner to avoid incorrect fault diagnostics. Therefore, for appropriate monitoring of a process, multiple sensors located at different places in the plant should be considered to detect a process fault.

The detection of changes in the process operation of a plant requires a monitoring technique that quantitatively represents the major relations among the process variables. Violation of such relations would indicate a potential malfunction in the plant. Principal-component analysis (PCA) (Jackson, 1980; Wold et al., 1987) is a reliable and simple technique for capturing variable correlation. Several articles have recently illustrated the use of PCA in process monitoring and statistical process control (Kresta et al., 1991; De Veaux, et al., 1995), fault diagnosis (Kourti and MacGregor, 1994; Raich and Cinar, 1994), and sensor validation (Tong and Crowe, 1995; Dunia et al., 1996a,b,c). The applications vary from batch processes (MacGregor et al., 1994) to continuous processes (Dunia and Qin, 1998). Miller et al. (1993) proposed a contribution plot approach based on PCA models to help identify variables strongly affected by the underlying fault.

Even though many authors have reported the success of using PCA for process monitoring, there are some fundamental issues related to statistical process monitoring that have not been developed in the PCA framework. For example, based on the confidence region used for fault detection, it is important to establish the minimum fault magnitude required

Correspondence concerning this article should be addressed to S. J. Qin.

for the appropriate detection and identification of a fault. Furthermore, it is important to determine if the PCA model is able to isolate one fault from others in order to diagnose the root causes of the fault. Such concepts are referred to as *detectability*, *reconstructability*, *identifiability*, and *isolatability* of a fault, which denote the capability of the fault diagnosis approach at different stages of fault monitoring. *Detectability* represents the capability of the model to detect the presence of a fault; *reconstructability* is a property that assures the estimation of the normal sample vector using the corrupted sample vector and the model; *identifiability* refers to the ability to find the true fault from a set of possible candidates; and *isolatability* makes faults capable of being distinguished from one another by means of the model and fault direction.

To determine how large a fault can be detected, it is convenient to parameterize the fault by its magnitude. Keller et al. (1994) have defined gross-error faults by the product of a vector (which specifies the faulty sensor) and a gross-error magnitude. Similarly, Dunia et al. (1996) made use of this representation for sensor fault reconstruction and identification via PCA. They provide a geometric approach to the monitoring problem by defining a partition of the measurement space into the model and residual subspaces, which can determine the data variations due to normal and abnormal operation conditions, respectively.

The fault parameterization in magnitude and direction was used by Dunia and Qin (1998) to quantitatively express the monitoring conditions for unidimensional process and sensor faults. In the unidimensional representation, a fault-direction vector in the measurement space is defined and reconstruction is done by sliding along the fault direction toward the principle-component subspace. A set of faults, which include sensor and process faults, was considered to determine if a fault can be detected, identified, reconstructed, and isolated using principal-component models. The PCA model was also determined such that the variance of the reconstructed error is minimized.

This work extends the concepts of detectability, identifiability, reconstructability, and isolatability to the multidimensional fault case, where the fault displacement occurs in a subspace. Fault identification is performed by reconstruction, which brings the sample vector back to the principal-component subspace along the subspace that describes the fault. The multidimensional nature of the fault makes it more difficult to derive the necessary and sufficient conditions. Because the dimensions of the fault subspace can be adjusted to best reconstruct the fault, the algorithm used to obtain the PCA model does not only consider the best model for fault reconstruction, but also provides the dimension of the fault subspace.

This article is organized in the following way. The next section presents the use of PCA for fault detection, and defines the conditions for fault detectability in terms of the fault basis and magnitude. The third section illustrates the fault reconstruction procedure when considering multidimensional fault subspaces. The concepts of complete and partial reconstruction are also introduced in this section to determine the capability of the PCA model to estimate the normal sample vector in the presence of a fault. The procedure to determine the model for best reconstruction is presented in the fourth section. This procedure makes use of the unreconstructed variance to determine (1) the optimal number of principal components, (2) the set of sensors to use for monitoring, and (3) the reconstructable directions in each fault subspace. These reconstructable directions specify the fault subspace dimension for identification and isolation. The identification of process faults is discussed in the fifth section. An identification index for multidimensional faults is also provided in this section. The sixth section derives the conditions for isolatability between a pair of faults. Isolatability can also be complete or partial depending on the fault subspace. A case study of a simulated process is given in the seventh section to illustrate the conditions for fault detectability, reconstructability, isolatability, and the selection of the number of principal components for best reconstruction. Finally, the eighth section provides a summary and conclusions of this article.

Fault Detection and Detectability

PCA and fault detection

Principal-component analysis decomposes a normalized sample vector into two portions,

$$\boldsymbol{x} = \hat{\boldsymbol{x}} + \tilde{\boldsymbol{x}}, \tag{1}$$

where $\boldsymbol{x} \in \Re^m$ is the sample vector normalized to zero mean and unit variance. The vectors $\hat{\boldsymbol{x}}$ and $\tilde{\boldsymbol{x}}$ are the modeled and residual portions of $\boldsymbol{x}$, respectively. The vector $\hat{\boldsymbol{x}}$ is the projection on the principal-component subspace (PCS):

$$\hat{\boldsymbol{x}} = \boldsymbol{P}\boldsymbol{t} = \boldsymbol{P}\boldsymbol{P}^T\boldsymbol{x} = \boldsymbol{C}\boldsymbol{x}, \tag{2}$$

where $\boldsymbol{P} \in \Re^{m \times l}$ is the PCA loading matrix, $\boldsymbol{t} \in \Re^l$ is the score vector, and $l \geq 1$ is the number of PCs retained in the PCA model. The matrix $\boldsymbol{C} \equiv \boldsymbol{P}\boldsymbol{P}^T$ represents the projection on the l = dimensional PCS, $\mathbb{S}$. Therefore, $\hat{\boldsymbol{x}} \in \mathbb{S} \subseteq \Re^m$, with $dim(\mathbb{S}) = l$.

The columns of the loading matrix, $\boldsymbol{P}$, are the eigenvectors of the correlation matrix ($\boldsymbol{R}$) associated with the l largest eigenvalues. For this reason, PCA captures the maximum measurement correlations of historical data under normal operation. The number of principal components (l) depends on the correlation among the process variables. Jackson (1991) summarized a few criteria for the selection of l. In the fourth section we propose a new method to calculate the number of principal components based on best fault reconstruction.

The residual $\tilde{\boldsymbol{x}}$ lies in the residual subspace (RS),

$$\tilde{\boldsymbol{x}} = (\boldsymbol{I} - \boldsymbol{C})\boldsymbol{x} = \tilde{\boldsymbol{C}}\boldsymbol{x} \in \tilde{\mathbb{S}} \subset \Re^m, \tag{3}$$

where $\tilde{\boldsymbol{C}} \equiv \boldsymbol{I} - \boldsymbol{C}$ represents the projection matrix on the RS, $\tilde{\mathbb{S}}$, with $dim(\tilde{\mathbb{S}}) = \tilde{l} = m - l$.

A change in variable correlation indicates an unusual situation, because the variables do not conserve their normal relations. Under this situation the sample $\boldsymbol{x}$ increases its projection to the RS. As a result, the magnitude of $\tilde{\boldsymbol{x}}$ reaches unusual values compared to those obtained during normal conditions. A typical statistic for detecting abnormal conditions is the squared prediction error (SPE),

$$\text{SPE} \equiv \| \tilde{\boldsymbol{x}} \|^2 = \| \tilde{\boldsymbol{C}}\boldsymbol{x} \|^2. \tag{4}$$

A confidence limit for SPE was originally developed by Jackson and Mudholkar (1979) and used later by many researchers (Wise and Ricker, 1991; MacGregor and Kourti, 1995; and Dunia et al., 1996a). The process is considered normal if

$$\text{SPE} \leq \delta^2, \tag{5}$$

where δ^2 denotes a confidence limit or threshold for the SPE.

Another index often used for fault detection is the Hotelling T^2 – test, which is described in, for example, Kresta et al. (1991). The T^2 index is defined as

$$T^2 = \boldsymbol{t}^T \boldsymbol{\Lambda}^{-1} \boldsymbol{t}, \tag{6}$$

which follows a χ^2 distribution of l degrees of freedom, where $\boldsymbol{\Lambda} = diag\{\lambda_1, \lambda_2, \ldots, \lambda_l\}$ is a diagonal matrix containing the l largest eigenvalues of the covariance matrix of $\boldsymbol{x}$. A multivariate χ^2 control chart can be obtained by plotting T^2 vs. time with a control limit $\chi^2_\beta(l)$, where β is the confidence level of the test. If $T^2 > \chi^2_\beta(l)$, an abnormal situation is indicated.

Definition of fault detectability

As discussed earlier, there are two typical indices for fault detection, the SPE and the T^2 indices. There can be as many as four cases for the two indices:

1. A fault in the process causes both SPE and T^2 to exceed the control limits.
2. A fault in the process causes SPE to exceed its control limit, but not T^2.
3. A fault in the process causes T^2 to exceed its control limit, but not SPE.
4. A fault in the process causes neither SPE nor T^2 to exceed the control limits.

It should be noted that, although SPE and T^2 indices are used in the literature to detect faults, they have different physical meanings and do not have the same importance in detecting faults. A PCA model, if built properly, extracts the correlation among variables due to mass balance, energy balance, and operational restrictions. A significant increase in SPE, which measures the distance from the PCS, indicates a breakdown of the normal correlation. Therefore, SPE detects faults that violate the process mass balance, energy balance, or operational restrictions. Using SPE index alone, one can consider fault cases 1, 2, and 4, regardless of the values for T^2. On the other hand, a significant increase in T^2 but no significant change in SPE, which is case 3, can be due to a fault or a normal change in the process throughput that conserves the correlation structure. Therefore, the use of T^2 could detect a fault that conserves that correlation structure, which could not be detected by SPE, but it also brings confusion with a normal change in throughput. The SPE detectability will cover three of the four cases previously listed. The T^2 detectability and how to discriminate a T^2-detectable fault from a normal throughput change deserve further study and will not be discussed in this article. For the remainder of the article, we refer to fault detectability, identifiability, and reconstructability in the sense of SPE only.

The SPE statistic is usually effective in detecting process or sensor faults. As indicated in case 4, however, some faults can happen in a way that does not affect the value of SPE. The situation is complicated when the fault is multidimensional. In the next subsection, we provide a general representation for multidimensional faults and derive the necessary and sufficient conditions for the detectability of multidimensional faults.

Necessary condition for detectability

The multidimensional-fault case considers the displacement of the operating point from the normal location (close to the PCS) into the fault subspace. We denote $\mathbb{S}_i$ as the subspace of fault $\mathcal{F}_i$, where $dim(\mathbb{S}_i) = l_i \leq m$ and $\mathbb{S}_i \subseteq \Re^m$. A set of bases for $\mathbb{S}_i$ can be represented as columns of $\boldsymbol{\Xi}_i \in \Re^{m \times l_i}$. In the case of a single fault with multiple dimensions, $\boldsymbol{\Xi}_i$ is chosen to be orthonormal. In the unidimensional fault case, $\boldsymbol{\Xi}_i$ reduces to a vector with unit norm. For the case of simultaneous unidimensional faults, the matrix composed by all unidimensional directions may not have linearly independent columns. However, we can always select a collection of independent directions to compose $\boldsymbol{\Xi}_i$. Singular-value decomposition (SVD) (Strang, 1980) can be applied to obtain an orthonormal basis for $\mathbb{S}_i$. For this reason, we assume that $\boldsymbol{\Xi}_i$ is orthonormal without loss of generality.

The sample vector for normal operating conditions is denoted by $\boldsymbol{x}^*$, which is unknown when a fault has occurred. In the presence of a process fault $\mathcal{F}_i$, the sample vector $\boldsymbol{x}$ is represented by the following expression:

$$\boldsymbol{x} = \boldsymbol{x}^* + \boldsymbol{\Xi}_i \boldsymbol{f}, \tag{7}$$

where $\boldsymbol{\Xi}_i$ is orthonormal and $\| \boldsymbol{f} \|$ represents the magnitude of the fault. Note that $\boldsymbol{f}$ may change over time depending on how the actual fault develops over time. The actual fault belongs to the set of possible faults, denoted by $\{\mathcal{F}_j\}$. Some members of this set may be combinations of faults.

The columns of $\boldsymbol{\Xi}_i$ can be projected onto $\mathbb{S}$ and $\tilde{\mathbb{S}}$:

$$\boldsymbol{\Xi}_i = \tilde{\boldsymbol{\Xi}}_i + \hat{\boldsymbol{\Xi}}_i, \tag{8}$$

where the columns of $\hat{\boldsymbol{\Xi}}_i \equiv \boldsymbol{C}\boldsymbol{\Xi}_i$ and $\tilde{\boldsymbol{\Xi}}_i \equiv \tilde{\boldsymbol{C}}\boldsymbol{\Xi}_i$ belong to $\mathbb{S}$ and $\tilde{\mathbb{S}}$, respectively. The following relation represents the projection of Eq. 7 onto $\tilde{\mathbb{S}}$,

$$\tilde{\boldsymbol{x}} = \tilde{\boldsymbol{x}}^* + \tilde{\boldsymbol{\Xi}}_i \boldsymbol{f}. \tag{9}$$

Although $\boldsymbol{\Xi}_i$ has full column rank, $\tilde{\boldsymbol{\Xi}}_i$ may not have full column rank. For this reason, we apply singular-value decomposition to $\tilde{\boldsymbol{\Xi}}_i$,

$$\begin{aligned} \tilde{\boldsymbol{\Xi}}_i &= [\tilde{\boldsymbol{U}}_i \; \boldsymbol{U}_i^\perp] \begin{bmatrix} \tilde{\boldsymbol{D}}_i \\ 0 \end{bmatrix} \begin{bmatrix} \tilde{\boldsymbol{V}}_i \; \tilde{\boldsymbol{V}}_i^\perp \end{bmatrix}^T \\ &= \tilde{\boldsymbol{U}}_i \tilde{\boldsymbol{D}}_i \tilde{\boldsymbol{V}}_i^T \\ &\equiv \tilde{\boldsymbol{\Xi}}_i^\circ \tilde{\boldsymbol{D}}_i \tilde{\boldsymbol{V}}_i^T, \end{aligned} \tag{10}$$

where $\tilde{U}_i^{\perp}$ and $\tilde{V}_i^{\perp}$ are orthogonal to $\tilde{\Xi}_i^{\circ} \equiv \tilde{U}_i \in \Re^{m \times \tilde{l}_i}$ and $\tilde{V}_i \in \Re^{l_i \times \tilde{l}_i}$, respectively. $\tilde{D}_i \in \Re^{\tilde{l}_i \times \tilde{l}_i}$ contains nonzero singular values of $\tilde{\Xi}_i$. Therefore, $\tilde{\Xi}_i^{\circ}$ represents the nonvanishing directions of $\tilde{\Xi}_i$, and $\tilde{U}_i^{\perp}$ the vanishing directions.

Equation 9 can be rewritten as

$$\tilde{x} = \tilde{x}^* + \tilde{\Xi}_i^{\circ} \tilde{D}_i V_i^T f \equiv \tilde{x}^* + \tilde{\Xi}_i^{\circ} \tilde{f}, \tag{11}$$

where

$$\tilde{f} \equiv \tilde{D}_i \tilde{V}_i^T f, \tag{12}$$

and

$$\| \tilde{f} \| = \| \tilde{\Xi}_i^{\circ} \tilde{f} \| = \| \tilde{\Xi}_i f \| \tag{13}$$

represents the fault displacement projected on $\tilde{\mathbb{S}}$. The columns of $\tilde{\Xi}_i$ and $\tilde{\Xi}_i^{\circ}$ span the same subspace $\tilde{\mathbb{S}}_i$, which is the projection of $\mathbb{S}_i$ on $\tilde{\mathbb{S}}$. The use of $\tilde{\Xi}_i^{\circ}$ instead of $\tilde{\Xi}_i$ eliminates the possibility of linear dependence of the fault basis projected onto $\tilde{\mathbb{S}}$.

From Eqs. 9 and 11, the SPE can be represented as follows:

$$\text{SPE} = \| \tilde{x}^* + \tilde{\Xi}_i f \|^2 = \| \tilde{x}^* + \tilde{\Xi}_i^{\circ} \tilde{f} \|^2. \tag{14}$$

If a fault happens but it does not affect the SPE, this fault cannot be detected by the SPE. Therefore, we have the following three cases as the necessary conditions for detectability:

(i) If $\tilde{\Xi}_i = \mathbf{0}$, the fault is not detectable no matter what f is.

(ii) If $\tilde{\Xi}_i \neq \mathbf{0}$, but $\tilde{\Xi}_i$ is rank deficient, that is, $0 < \tilde{l}_i < l_i$, the fault is not detectable if $f \in \Re(\tilde{V}_i^T) = \Re(\tilde{V}_i^{\perp})$, which makes $\tilde{f} = \mathbf{0}$ from Eq. 12.

(iii) If $\tilde{f} \neq \mathbf{0}$, the fault is detectable, which implies one of the following situations: (a) $\tilde{\Xi}_i$ has full column rank, or $\tilde{l}_i = l_i$ or (b) $f \notin \Re(\tilde{V}_i^T) = \Re(\tilde{V}_i^{\perp})$. These conditions can be easily verified with Eq. 14. Intuitively, condition (i) implies that $\mathbb{S}_i \subseteq \mathbb{S}$. Condition (ii) indicates that the displacement caused by $\Xi_i f$ in Eq. 7 is part of the normal variation of the process variables, that is, $\Xi_i f \in \mathbb{S}$. Note that the case of $\mathbb{S} \subset \mathbb{S}_i$ does not prohibit the detection of $\mathcal{F}_i$, but is possible that $\Xi_i f \in \mathbb{S}$, which is undetectable.

Figure 1 illustrates the necessary condition for fault detection. The measurement space $\Re^m$ is partitioned into $\mathbb{S}$ and $\tilde{\mathbb{S}}$. In the top figure, $\mathbb{S}_i$ is represented by a circular region, and is decomposed into $\tilde{\mathbb{S}}_i = \mathbb{S}_i \cap \tilde{\mathbb{S}}$ and $\hat{\mathbb{S}}_i = \mathbb{S}_i \cap \mathbb{S}$. If f is such that $\Xi_i f \in \hat{\mathbb{S}}_i$, $\mathcal{F}_i$ is not detectable, otherwise $\mathcal{F}_i$ is detectable. In the bottom figure, $\mathcal{F}_i$ is not detectable regardless of the magnitude and direction of f.

Sufficient condition for detectability

The preceding section shows that the necessary condition for a fault to be detectable is that its projection on $\tilde{\mathbb{S}}$ does not vanish, that is, $\| \tilde{f} \| \neq 0$. Nevertheless, $\| \tilde{f} \|$ should be large enough to make the SPE exceed the confidence limit, that is, SPE $> \delta^2$. This detectability requirement on $\| \tilde{f} \|$ can be obtained using the following inequality:

$$\| \tilde{x} \| = \| \tilde{x}^* + \tilde{\Xi}_i^{\circ} \tilde{f} \| \geq \| \tilde{f} \| - \| \tilde{x}^* \|. \tag{15}$$

Since $\| \tilde{x}^* \|^2$ is the SPE for the normal data, $\| \tilde{x}^* \| \leq \delta$, which defines the normal region. Therefore,

$$\| \tilde{x} \| \geq \| \tilde{f} \| - \delta. \tag{16}$$

To make the fault sufficiently detectable, we must have SPE $= \| \tilde{x} \|^2 > \delta^2$, which requires $\| \tilde{f} \| > 2\delta$. Therefore, *a fault $\mathcal{F}_i$ is guaranteed detectable (with a confident limit) if*

$$\| \tilde{f} \| > 2\delta. \tag{17}$$

In other words, *the fault magnitude projected on the RS has to be larger than the diameter of the confidence region.*

The preceding inequality gives a sufficient condition for detectability. The following remarks should be made:

- The condition $\tilde{f} \neq 0$ is necessary for detectability.
- $\| \tilde{f} \| > 2\delta$ is a sufficient condition for detectability. Therefore, if this condition is satisfied, it is guaranteed that the fault will be detected.
- If $0 < \| \tilde{f} \| \leq 2\delta$, the fault may be detected, but not guaranteed detectable.
- To make small faults detectable, it is desirable to reduce δ, which means to use as many PCs as possible. However,

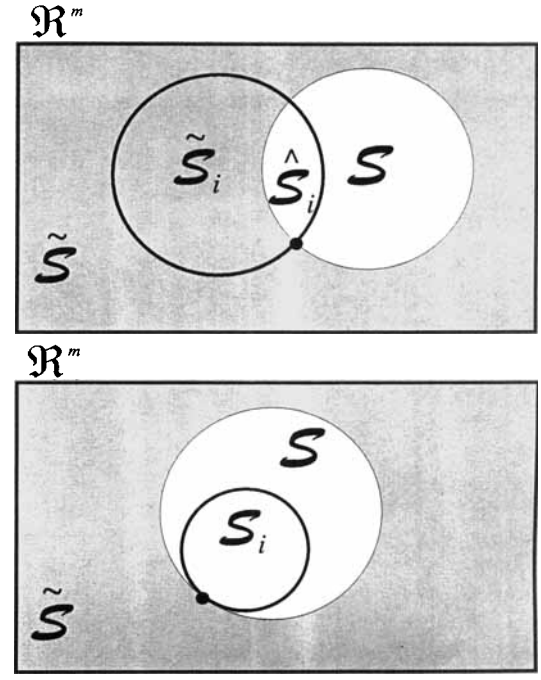

Figure 1. $\Re^m$ is partitioned into $\mathbb{S}$ (white) and $\tilde{\mathbb{S}}$ (gray background).

The point ● represents the null space. $\mathbb{S}_i = \tilde{\mathbb{S}}_i \cup \hat{\mathbb{S}}_i$ is represented by a circular region (top). If $\mathbb{S}_i = \hat{\mathbb{S}}_i$ (bottom), $\mathcal{F}_i$ is not detectable.

using more PCs reduces $\| \tilde{f} \|$, which tends to make the fault less detectable. There is actually a trade-off to determine the optimum number of PCs.

Fault Reconstruction and Reconstructability

Fault reconstruction

In the previous section we have presented the conditions for sufficient and necessary detectability of a process fault. When a fault is detected, it is desirable to determine the necessary adjustments to bring the process back to normal condition. This will also provide an estimate of the fault magnitude. To conduct reconstruction, we first need to identify the fault. In this section, we assume the actual fault has been identified as $\mathcal{F}_i$ and try to reconstruct the normal portion (x^*) from the corrupted vector (x) and the PCA model. The identification procedure is discussed later in this article.

The reconstruction of process faults consists of estimating the reconstructed sample vector x_i by eliminating the effect of the fault $\mathcal{F}_i$,

$$x_i = x - \Xi_i f_i, \tag{18}$$

where f_i is an estimate of the fault displacement, f. Geometrically, we would like to bring x_i back to the PCS along the fault basis, Ξ_i, as shown in Figure 2. Projecting Eq. 18 to $\tilde{S}$ and using Eq. 10.

$$\begin{aligned} \tilde{x}_i &= \tilde{x} - \tilde{\Xi}_i f_i \\ &= \tilde{x} - \tilde{\Xi}_i^{\circ} \tilde{f}_i, \end{aligned} \tag{19}$$

where

$$\tilde{f}_i = \tilde{D}_i \tilde{V}_i^T f_i \tag{20}$$

is the projection of the fault on $\tilde{\mathcal{S}}$.

The best estimate of x^* is found by minimizing the distance from x_i to the RS, that is, $\| \tilde{x}_i \|$. Therefore, the reconstruction is given by finding f_i:

$$f_i = \arg\min \| \tilde{x} - \tilde{\Xi}_i f_i \|^2 \tag{21}$$

$$= \left(\tilde{\Xi}_i^T \tilde{\Xi}_i \right)^{-1} \tilde{\Xi}_i^T \tilde{x}. \tag{22}$$

From Eq. 22 note that f_i can be uniquely calculated if and only if $(\tilde{\Xi}_i^T \tilde{\Xi}_i)^{-1}$ exists, that is, $\dim\{\tilde{\mathcal{S}}_i\} = l_i$. This condition indicates that the dimension of $\mathcal{F}_i$ does not decrease after projecting onto the PCS. In this case $\tilde{\Xi}_i$ has full column rank, $\tilde{\Xi}_i^T \tilde{\Xi}_i$ is invertible, and all the dimensions in $\mathcal{S}_i$ can be reconstructed. We refer to this case as the *complete reconstruction*, since all the dimensions can be reconstructed. However, in some cases the fault cannot be completely reconstructed because $\tilde{\Xi}_i^T \tilde{\Xi}_i$ is not invertible. In this case, there is no unique solution for f_i. Such a fault can only be *partially* reconstructed and the effect of the fault is partially corrected.

We will derive the necessary and sufficient conditions for complete and partial reconstructability. Such conditions allow one to assess the feasibility of fault reconstruction.

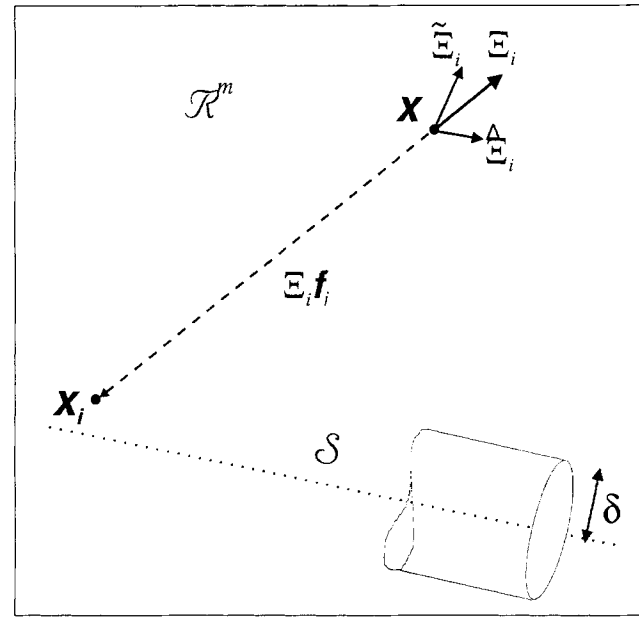

Figure 2. Fault reconstruction: the reconstructed vector x_i is obtained by taking x (- - - -) toward $\mathcal{S}$(· · · · · ·) in direction Ξ_i.

Complete reconstructability

Equation 18 illustrates that the feasible calculation of f_i makes the calculation of x_i feasible. Furthermore, because the fault basis is orthogonal, there exists a one-to-one correspondence between x_i and f_i in Eq. 18. Therefore, the condition for the uniqueness of f_i in Eq. 21 corresponds to the condition for complete reconstructability of x^*. As a consequence, the necessary and sufficient condition for *complete reconstructability* is any one of the following statements:

(i) $\dim\{\tilde{\mathcal{S}}_i\} = \dim\{\mathcal{S}_i\} = l_i$;

(ii) $\mathcal{S}_i \cap \mathcal{S} = \mathbf{0}$;

(iii) $\tilde{\Xi}_i$ has full column rank;

(iv) $\sigma_{\min}(\tilde{\Xi}_i) > 0$, where $\sigma_{\min}(\tilde{\Xi}_i)$ is the smallest singular value of $\tilde{\Xi}_i$.

Figure 3 illustrates the case of complete reconstructability of fault $\mathcal{S}_i$. The intersection between $\mathcal{S}_i$ and $\mathcal{S}$ is the null vector, represented by •.

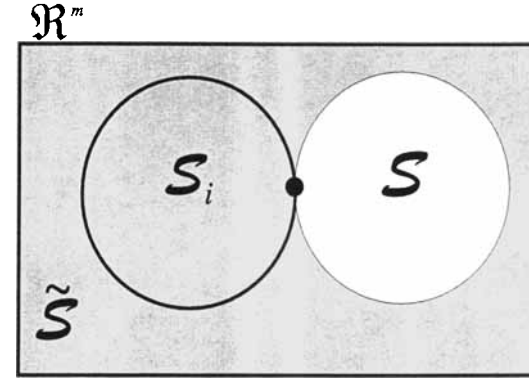

Figure 3. The fault $\mathcal{S}_i$ is completely reconstructed because $\mathcal{S}_i \cap \mathcal{S} = \mathbf{0}$.

Substitution of Eq. 22 in Eq. 18 provides the expression for x_i,

$$x_i = x - \Xi_i\left(\tilde{\Xi}_i^T\tilde{\Xi}_i\right)^{-1}\tilde{\Xi}_i^T\,\tilde{x} = \left[I - \Xi_i\left(\tilde{\Xi}_i^T\tilde{\Xi}_i\right)^{-1}\tilde{\Xi}_i^T\tilde{C}\right]x$$
$$= \left[I - \Xi_i\left(\tilde{\Xi}_i^T\tilde{\Xi}_i\right)^{-1}\tilde{\Xi}_i^T\right]x, \tag{23}$$

and its projection on $\tilde{\mathbb{S}}$ is given by

$$\tilde{x}_i = \left[\tilde{C} - \tilde{\Xi}_i\left(\tilde{\Xi}_i^T\tilde{\Xi}_i\right)^{-1}\tilde{\Xi}_i^T\right]x$$
$$= \left[I - \tilde{\Xi}_i\left(\tilde{\Xi}_i^T\tilde{\Xi}_i\right)^{-1}\tilde{\Xi}_i^T\right]\tilde{x}. \tag{24}$$

Partial reconstructability

When a fault is not completely reconstructable, some dimensions in $\mathbb{S}_i$ vanish after projection on $\tilde{\mathbb{S}}$. This is the case where $\tilde{\Xi}_i$ is rank-deficient. However, we can compute a *partial reconstruction* by finding a minimum norm solution to Eq. 21 using the Moore–Penrose pseudoinverse (Albert, 1972). Appendix A shows that a minimum norm solution to Eq. 21 is

$$f_i = \tilde{\Xi}_i^+\tilde{x} = \tilde{\Xi}_i^+x, \tag{25}$$

where the Moore–Penrose pseudoinverse using the SVD form of Eq. 10 is,

$$\tilde{\Xi}_i^+ = \tilde{V}_i\tilde{D}_i^{-1}\tilde{\Xi}_i^{\circ T}. \tag{26}$$

Equation 20 now becomes

$$\tilde{f}_i = \tilde{D}_i\tilde{V}_i^Tf_i = \tilde{\Xi}_i^{\circ T}\tilde{x} = \tilde{\Xi}_i^{\circ T}x. \tag{27}$$

The reconstructed vector is obtained by the substitution of Eq. 25 into Eq. 18,

$$x_i = (I - \Xi_i\tilde{\Xi}_i^+)x, \tag{28}$$

or by the substitution of Eq. 27 into Eq. 19,

$$\tilde{x}_i = \left(I - \tilde{\Xi}_i^{\circ}\tilde{\Xi}_i^{\circ T}\right)\tilde{x}. \tag{29}$$

From the preceding equations we notice that f_i and x_i can be calculated as long as $\tilde{\Xi}_i \neq \mathbf{0}$. Therefore, a fault is *partially reconstructable* if and only if $\tilde{\Xi}_i \neq \mathbf{0}$ is any one of the following statements:

(i) $\dim\{\tilde{\mathbb{S}}_i\} \neq 0$;

(ii) $\mathbb{S}_i \not\subseteq \mathbb{S}$;

(iii) $\tilde{\Xi}_i \neq \mathbf{0}$; or

(iv) $\sigma_{\max}(\tilde{\Xi}_i) > 0$, where $\sigma_{\max}(\tilde{\Xi}_i)$ is the largest singular value of $\tilde{\Xi}_i$.

Figure 1 can be used to illustrate the case for partially reconstructable faults (top) and unreconstructable faults (bottom), where $\mathbb{S}_i \subseteq \mathbb{S}$. In most circumstances the condition for partial reconstructability is easy to satisfy because it is a coincidence to have $\mathbb{S}_i \subseteq \mathbb{S}$.

Complete vs. partial reconstruction

The cases for complete reconstruction and partial reconstruction are fundamentally different. In the case of complete reconstruction, where $\tilde{\Xi}_i$ has full column rank, all directions can be reconstructed. In the case of partial reconstruction, however, only the nonvanishing directions projected on $\tilde{\mathbb{S}}$ can be reconstructed. However, *complete reconstruction is a special case for partial reconstruction*, since

$$\tilde{\Xi}_i^+ = \left(\tilde{\Xi}_i^T\tilde{\Xi}_i\right)^{-1}\tilde{\Xi}_i^T, \tag{30}$$

if $\tilde{\Xi}_i$ has full column rank. Therefore, Eqs. 25, 27, 28, and 29 reduce to Eqs. 22, 20, 23, and 24, respectively, and are applicable to both complete and partial reconstruction. In the subsequent sections of the article, we will use the formulas for partial reconstruction to represent the general case.

The conditions for partial and complete reconstruction can be summarized as follows:

(i) If $\tilde{\Xi}_i = \mathbf{0}$, the fault is not reconstructable.

(ii) If $0 < \text{rank}(\tilde{\Xi}_i) = \tilde{l}_i < l_i$, the fault is partially reconstructable.

(iii) If $\text{rank}(\tilde{\Xi}_i) = l_i$, the fault is completely reconstructable, that is, all the fault directions can be corrected or reconstructed.

(iv) If $\tilde{\Xi}_i \neq \mathbf{0}$, but $f \in \mathfrak{N}\{\tilde{\Xi}_i\}$, the fault occurs in the vanishing directions of $\tilde{\Xi}_i$. In this case, although the fault is partially reconstructable, it is not detectable. Here rank means rank of a matrix.

Model for Best Reconstruction

In order to achieve the best fault reconstruction, we need to select the optimal number of principal components and an appropriate set of variables for monitoring. In this section we propose a quantitative criterion that estimates the goodness of the reconstruction, x_i. We present the *unreconstructed variance* as the indicator that determines how reliable the reconstructed sample vector is for different sets of sensors and principal components.

Unreconstructed variance

Dunia et al. (1996a) defined the unreconstructed variance for a single sensor fault, which measures the reliability of the reconstruction procedure. This notion was extended to the case of unidimensional process faults, in which reconstruction is accomplished on a fault direction (Dunia and Qin, 1996). Here we present a general definition of the unreconstructed variance of faults characterized by a subspace for complete and partial reconstruction of a multidimensional fault.

In the case of a multidimensional fault $\mathfrak{F}_i$, we reconstruct the whole set of measurements x^* using the fault basis Ξ_i. The unreconstructed portion of x^* is $x^* - x_i \in \mathbb{S}_i$. We define the *unreconstructed mean* and the *unreconstructed vari-*

ance as the mean and variance of the unreconstructed portion in $\mathcal{S}_i$, respectively,

$$w_i \equiv \mathcal{E}\{\Xi_i^T(x^* - x_i)\} \tag{31}$$

$$u_i \equiv \text{var}\{\Xi_i^T(x^* - x_i)\} = \mathcal{E}\{\| \Xi_i^T(x^* - x_i) - w_i \|^2\}. \tag{32}$$

Substituting Eq. 7 in Eq. 18 gives:

$$x^* - x_i = \Xi_i(f_i - f). \tag{33}$$

Therefore,

$$w_i = \mathcal{E}\{f_i - f\} \tag{34}$$

$$u_i = \mathcal{E}\{\| f_i - f - w_i \|^2\}. \tag{35}$$

To calculate the unreconstructed mean and variance, we consider the general case of partial reconstruction and that the fault magnitude is deterministic, that is, $\mathcal{E}\{f\} = f$. Substituting Eq. 25 in Eq. 34 yields

$$\begin{aligned} w_i &= \mathcal{E}\{\tilde{\Xi}_i^+(x^* + \Xi_i f) - f\} \\ &= (\tilde{\Xi}_i^+ \Xi_i - I) f \\ &= \left(\tilde{\Xi}_i^+ \tilde{\Xi}_i - I\right) f. \end{aligned} \tag{36}$$

In this case, x_i is a biased estimation of x^*. Similarly, substitution of Eqs. 25 and 36 into Eq. 35 leads to

$$\begin{aligned} u_i &= \mathcal{E}\{\| \tilde{\Xi}_i^+(x^* + \Xi_i f) - f - (\tilde{\Xi}_i^+ \Xi_i - I) f \|^2\} \\ &= \mathcal{E}\{\| \tilde{\Xi}_i^+ x^* \|^2\} \\ &= \text{trace}\left\{\tilde{\Xi}_i^+ R \tilde{\Xi}_i^{+T}\right\}, \end{aligned} \tag{37}$$

where the relation $a^T a = \text{trace}\{aa^T\}$ is used, and *trace* means trace of a matrix.

In the case of complete reconstruction, Eq. 36 becomes

$$w_i = \left(\left(\tilde{\Xi}_i^T \tilde{\Xi}_i\right)^{-1} \tilde{\Xi}_i^T \tilde{\Xi}_i - I\right) f = 0.$$

Therefore, the reconstruction is unbiased for the case of complete reconstruction. For the case of partial reconstruction, where $\tilde{\Xi}_i$ is rank-deficient, a bias is incurred to achieve a minimum norm estimation of f. This minimum norm estimation has meaningful implications in fault identification, to be discussed in the next section.

Number of principal components for best reconstruction

As indicated in Eq. 37, u_i does not depend on the magnitude of the fault. Therefore, to minimize the unreconstructed variance u_i, we consider the fault-free cases only, or, $f = 0$, in Eq. 35,

$$\begin{aligned} u_i &= \mathcal{E}\{\| f_i \|^2\} = \mathcal{E}\{\| \Xi_i f_i \|^2\} \\ &= \mathcal{E}\left\{\| \left(\tilde{\Xi}_i + \hat{\Xi}_i\right) f_i \|^2\right\} \\ &= \mathcal{E}\{\| \tilde{\Xi}_i f_i \|^2\} + \mathcal{E}\{\| \hat{\Xi}_i f_i \|^2\} \\ &\equiv \tilde{u}_i + \hat{u}_i, \end{aligned} \tag{38}$$

where

$$\tilde{u}_i \equiv \mathcal{E}\{\| \tilde{\Xi}_i f_i \|^2\} = \text{var}\{\tilde{\Xi}_i f_i\} \tag{39}$$

is the variance of f_i projected on $\tilde{\mathcal{S}}$, and

$$\hat{u}_i \equiv \mathcal{E}\{\| \hat{\Xi}_i f_i \|^2\} = \text{var}\{\hat{\Xi}_i f_i\} \tag{40}$$

is the variance of f_i projected on $\hat{\mathcal{S}}$. The relation $\hat{\Xi}_i^T \tilde{\Xi}_i = 0$ is applied in deriving the preceding relations.

Figure 4 (top) shows the projection of x^* and x_i (grey dots) on $\mathcal{S}$ (white dots) and $\tilde{\mathcal{S}}$ (black dots), which allows one to visualize the projection of $x^* - x_i$ on these subspaces. The fault basis Ξ_i is decomposed into $\hat{\Xi}_i$ and $\tilde{\Xi}_i$, which corresponds to the projections onto $\mathcal{S}$ and $\tilde{\mathcal{S}}$, respectively. The difference $\tilde{x}^* - \hat{x}_i$ is in $\mathcal{S}$ and can be represented by $\hat{\Xi}_i f_i$, while $\tilde{x}^* - \hat{x}_i$ is in $\tilde{\mathcal{S}}$ and is given by $\tilde{\Xi}_i f_i$.

The expectations of $\| \hat{x}^* - \hat{x}_i \|^2$ and $\| \tilde{x}^* - \hat{x}_i \|^2$ represent $\hat{u}_i$ and $\tilde{u}_i$, respectively. Figure 4 (bottom) shows how

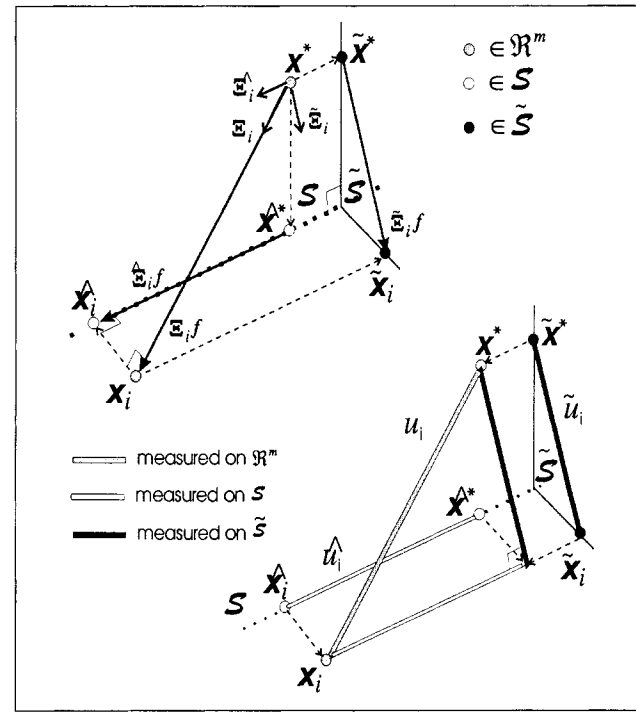

Figure 4. Projection of the unreconstructed variance on the PCS and RS.

Top: the points $\mathbf{x}^*$ and $\mathbf{x}_i$ are in $\Re^m$ and their difference is given by the displacement $\Xi_i f_i$. The displacement is projected onto $\mathcal{S}$ and $\tilde{\mathcal{S}}$, resulting in $\hat{\Xi}_i f_i$ and $\tilde{\Xi}_i f_i$, respectively. Bottom: the expected squared-norm of these projections represents the unreconstructed variances measured on $\mathcal{S}$ and $\tilde{\mathcal{S}}$.

$\hat{u}_i$ (white bar), $\tilde{u}_i$ (black bar), and u_i (grey bar) are related. The index u_i corresponds to the hypotenuse (gray bar), while $\hat{u}_i$ and $\tilde{u}_i$ correspond to the adjacent sides of the 90° angle.

Next we show that the addition of $\tilde{u}_i(l)$ and $\hat{u}_i(l)$ provides the possibility for a minimum with respect to l. Equation 39 can be rewritten as follows using Eq. 27,

$$\begin{aligned}\tilde{u}_i &= \mathcal{E}\left\{\| \tilde{\Xi}_i^{\circ} \tilde{f}_i \|^2\right\} = \mathcal{E}\{\| \tilde{f}_i \|^2\} \\ &= \mathcal{E}\left\{x^{*T} \tilde{\Xi}_i^{\circ} \tilde{\Xi}_i^{\circ T} x^*\right\} \\ &= \operatorname{trace}\left\{\tilde{\Xi}_i^{\circ T} R \tilde{\Xi}_i^{\circ}\right\} = \sum_{j=1}^{\tilde{l}_i} \tilde{\xi}_{ij}^{\circ T} R \tilde{\xi}_{ij}^{\circ}. \end{aligned} \tag{41}$$

The unit norm vector $\tilde{\xi}_{ij}^{\circ}$ represents the jth column of $\tilde{\Xi}_i^{\circ}$. Dunia and Qin (1998) have demonstrated that $\tilde{\xi}_{ij}^{\circ T} R \tilde{\xi}_{ij}^{\circ}$ is monotonically decreasing with respect to l. Therefore, the summation in Eq. 41 is also monotonically decreasing with respect to l, and results in $\tilde{u}_i$. Intuitively, the larger the number of PCs, the smaller are the nonzero eigenvalues remaining in $\tilde{R}$, making $\tilde{u}_i(l+1) \le \tilde{u}_i(l)$.

The expression for $\hat{u}_i$ is given by Eqs. 40 and 25:

$$\begin{aligned}\hat{u}_i &= \mathcal{E}\left\{\| \hat{\Xi}_i \tilde{\Xi}_i^{+} x \|^2\right\} \\ &= \operatorname{trace}\left\{\hat{\Xi}_i \tilde{\Xi}_i^{+} R \tilde{\Xi}_i^{+T} \hat{\Xi}_i^{T}\right\}. \end{aligned} \tag{42}$$

For $l \to m$, $\mathcal{S} \to \Re^m$ and $x_i \to \Re^m$ have a small distance to $\mathcal{S}$. As a result, its variance $\hat{u}_i$ is large.

Figure 5 illustrates the effect of l on u_i, $\tilde{u}_i$, and $\hat{u}_i$, represented by the grey, black, and white bars, respectively. The subplots in Figure 5a and 5c show the unreconstructed variance for the same number of principal components. The increase of l tends to move the fault subspace $\mathcal{S}_i$ and the normal sample vector x closer to $\mathcal{S}$, as is shown in the subplots in Figure 5b and 5d. The resulting $\tilde{u}_i$ is monotonically decreasing with l. However, the projection $\hat{u}_i$ on $\mathcal{S}$ can decrease or increase with l, as it decreases in the subplot in Figure 5b and increases in Figure 5d. Therefore, $\hat{u}_i$ is not necessarily monotonically increasing with l. Nevertheless, the subplot in Figure 5e shows that the tendency when $l \to m$ is to have a fault subspace almost included in the PCS, which makes the projection of the unreconstructed variance on $\mathcal{S}$ large.

Because $\tilde{u}_i$ is monotonically decreasing with respect to l, and $\hat{u}_i$ is large when $l \to m$, the sum $\tilde{u}_i + \hat{u}_i = u_i$ provides the existence of a minimum with respect to l. The calculation of a minimum u_i by choosing l improves reconstruction and identification of $\mathcal{F}_i$. Therefore, we formulate an optimization problem where the objective is to minimize a linear combination of all possible u_i with respect to the number of principal components,

$$\min_l q^T u = \min_l (q^T \tilde{u} + q^T \hat{u}), \tag{43}$$

where u represents the vector of the unreconstructed variances for all $\mathcal{F}_i \in \{\mathcal{F}_j\}$, and q is a weighting vector with positive entries. Such a vector allows one to adjust the model,

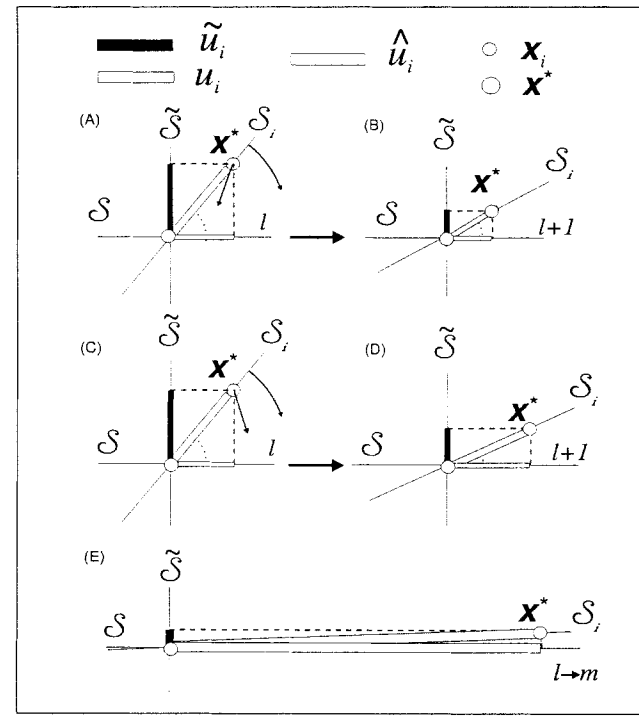

Figure 5. Effect of l on u_i, $\tilde{u}_i$, and $\hat{u}_i$.

The subplots (a) and (c) represent the unreconstructed variances under the same number of principal components. When l is increased, the projection $\hat{u}_i$ can decrease or increase, as illustrated in the subplots (b) and (d), respectively. Nevertheless, $\tilde{u}_i$ always decreases with l. Finally, the subplot (e) illustrates the tendency of the unreconstructed variances for $l \to m$. In this situation $\hat{u}_i$ is large because $\mathcal{S}_i$ is almost included in $\mathcal{S}$.

depending on how critical each fault is to process operation. Note that the linear combination of monotonically decreasing functions $q^T\tilde{u}$ is also monotonically decreasing, and $q^T\hat{u}$ is large when $l \to m$. Therefore, a minimum also exists for $q^T u$.

Inclusion of faults and variables

The reconstructability condition only shows the feasibility to calculate x_i from the PCA model given a fault bias Ξ_i. If there is a lack of correlation among all variables, however, it is possible that the best reconstruction is not better than the sample mean, $\bar{x}_i$. In other words, denoting the unreconstructed variance using the sample mean as

$$\begin{aligned}\varrho_i &\equiv \mathcal{E}\{\| \Xi_i^T (x^* - \bar{x}^*) \|^2\} = \operatorname{var}\{\Xi_i^T x^*\} \\ &= \operatorname{trace}\{\Xi_i^T R \Xi_i\}, \end{aligned} \tag{44}$$

it is possible to have $u_i > \varrho_i$. In this case, it is desirable to take the following options to reduce the reconstructed variance:

1. Reduce the variance u_i by dropping out insignificant singular values of $\tilde{\Xi}_i$ that tend to introduce large reconstruction variance.

2. If after the preceding step we still have $u_i > \varrho_i$, the fault $\mathcal{F}_i$ cannot be *reliably* reconstructed using the PCA model, and the best reconstruction is the sample mean. Such faults should

not be reconstructed using correlation-based methods, such as PCA.

3. If $\mathcal{F}_i$ is a sensor fault that cannot be *reliably* reconstructed, that sensor has little correlation with others and should be removed from the PCA model. The monitoring of that sensor fault can be done using univariate methods since it is essentially independent of others. Inclusion of such sensors tend to inflate the unreconstructed variance $\boldsymbol{q}^T\boldsymbol{u}$, which is not desirable.

The preceding options provide an iterative approach to determining:

(i) The significant dimension of a fault subspace at a varying number of principal components;

(ii) The set of faults to be reliably reconstructed using the PCA model;

(iii) The set of variables to be included in the PCA model with significant correlation;

(iv) The number of components for best reconstruction for the selected set of variables and faults. Faults that are excluded during this procedure can only be reconstructed using other methods such as using the sample mean.

The previous discussion suggests the following procedure for the selection of m and l using the unreconstructed variance:

1. Start with $l = 1$ in the first iteration.
2. Consider all monitoring sensors.
3. Estimate the correlation matrix $\boldsymbol{R}$ from normal process data.
4. Calculate a principal-component model.
5. Calculate the unreconstructed variance for sensor faults only.
6. If for sensor i such that $u_i > \varrho_i = 1$, the sensor is taken out from the set of variables used for monitoring. In this case, return to step 3 until no sensor is eliminated.
7. Adjust the process fault descriptions, $\{\boldsymbol{\Xi}_i\}$, based on the set of sensors selected for monitoring.
8. Calculate the unreconstructed variance for process faults.
9. If $u_i > \varrho_i$, the direction in $\boldsymbol{\Xi}_i$ with the smallest singular value is dropped out (partial reconstruction). u_i and ϱ_i are recalculated until $u_i < \varrho_i$. If all the directions in $\mathcal{S}_i$ provide a poor reconstruction, $\mathcal{F}_i$ is taken out from the set of faults to be identified.
10. If all sensors were eliminated in step 6, l is too large for the number of selected sensors, and the iteration stops. Otherwise, calculate $\boldsymbol{q}^T\boldsymbol{u}$, increment l by one, and return to step 2.
11. Determine at which l the parameter $\boldsymbol{q}^T\boldsymbol{u}$ is minimum. This provides not only the optimal l, but also the best set of sensors for monitoring.

Fault Identification

Once a fault is detected, the next task is to identify it from a set of possible faults $\{\mathcal{F}_j, j = 1, \ldots, J\}$. In this article, the identification of a fault is carried out by assuming each of the faults in $\{\mathcal{F}_j\}$ in turn and performing reconstruction. When the actual fault $\mathcal{F}_i$ is assumed, the reconstructed sample vector $\boldsymbol{x}_i$ is closest to the PCS, and the SPE of $\boldsymbol{x}_i$ is brought in the normal confidence region. On the other hand, if $\mathcal{F}_j$ $(j \neq i)$ is assumed and the SPE of $\boldsymbol{x}_{j\neq i}$ is larger than the normal confidence region, then $\mathcal{F}_j$ is rejected as the possible fault. We define the SPE of $\boldsymbol{x}_j$ as follows:

$$\mathrm{SPE}_{j|i} = \| \tilde{\boldsymbol{x}}_j \|^2, \tag{45}$$

given that $\mathcal{F}_i$ is the actual fault. If the actual fault $\mathcal{F}_i$ is assumed, the SPE is brought within the normal confidence region:

$$\mathrm{SPE}_{i|i} = \| \tilde{\boldsymbol{x}}_i \|^2 \leq \delta_i^2. \tag{46}$$

Due to the fact that reconstruction is involved in $\mathrm{SPE}_{i|i}$, δ_i^2 is necessarily different from δ^2 where no reconstruction is involved. In the remaining part of this section, we discuss the relation of δ_i with δ, the identification procedures, and an identification index that can be used to identify the actual fault.

Relationship between δ_i and δ

Substituting Eq. 29 into $\mathrm{SPE}_{j|i}$, we obtain:

$$\mathrm{SPE}_{j|i} = \| \left(\boldsymbol{I} - \tilde{\boldsymbol{\Xi}}_j^{\circ} \tilde{\boldsymbol{\Xi}}_j^{\circ T} \right) \tilde{\boldsymbol{x}} \|^2 \tag{47}$$

$$= \| \left(\boldsymbol{I} - \tilde{\boldsymbol{\Xi}}_j^{\circ} \boldsymbol{\Xi}_j^{\circ T} \right) \left(\tilde{\boldsymbol{x}}^* + \tilde{\boldsymbol{\Xi}}_i^{\circ} \tilde{\boldsymbol{f}} \right) \|^2. \tag{48}$$

If $j = i$,

$$\begin{aligned} \mathrm{SPE}_{i|i} &= \| \left(\boldsymbol{I} - \tilde{\boldsymbol{\Xi}}_i^{\circ} \tilde{\boldsymbol{\Xi}}_i^{\circ T} \right) \left(\tilde{\boldsymbol{x}}^* + \tilde{\boldsymbol{\Xi}}_i^{\circ} \tilde{\boldsymbol{f}} \right) \|^2 \\ &= \| \left(\boldsymbol{I} - \tilde{\boldsymbol{\Xi}}_i^{\circ} \tilde{\boldsymbol{\Xi}}_i^{\circ T} \right) \tilde{\boldsymbol{x}}^* + \tilde{\boldsymbol{\Xi}}_i^{\circ} \tilde{\boldsymbol{f}} - \tilde{\boldsymbol{\Xi}}_i^{\circ} \tilde{\boldsymbol{f}} \|^2 \\ &= \| \left(\boldsymbol{I} - \tilde{\boldsymbol{\Xi}}_i^{\circ} \boldsymbol{\Xi}_i^{\circ T} \right) \tilde{\boldsymbol{x}}^* \|^2. \end{aligned} \tag{49}$$

Note that the $\mathrm{SPE}_{i|i}$ is not a function of the actual fault magnitude f. Therefore, the confidence region for $\mathrm{SPE}_{i|i}$ remains the same regardless of the fault magnitude, f. Consequently, we can calculate the confidence limit δ_i *a priori* based on the fault-free case along all fault directions $\{\boldsymbol{\Xi}_i, i = 1, 2, \ldots\}$. Such a confidence limit is still valid when a fault has happened.

We denote $\mathrm{SPE}_{i|0}$ as the SPE of $\boldsymbol{x}_i$ when there is no fault, which has the same form as $\mathrm{SPE}_{i|i}$:

$$\begin{aligned} \mathrm{SPE}_{i|0} &= \| \left(\boldsymbol{I} - \tilde{\boldsymbol{\Xi}}_i^{\circ} \tilde{\boldsymbol{\Xi}}_i^{\circ T} \right) \tilde{\boldsymbol{x}}^* \|^2 \\ &= \tilde{\boldsymbol{x}}^{*T} \left(\boldsymbol{I} - \tilde{\boldsymbol{\Xi}}_i^{\circ} \tilde{\boldsymbol{\Xi}}_i^{\circ T} \right) \tilde{\boldsymbol{x}}^* \\ &= \| \tilde{\boldsymbol{x}}^* \|^2 - \| \tilde{\boldsymbol{f}}_i \|^2 \\ &= \mathrm{SPE} - \| \tilde{\boldsymbol{f}}_i \|^2. \end{aligned} \tag{50}$$

Equation 27 is used in deriving the preceding relation. Since

$$\mathrm{SPE} = \| \tilde{\boldsymbol{x}}^* \|^2 \leq \delta^2, \tag{51}$$

we obtain

$$\mathrm{SPE}_{i|0} \leq \delta^2 - \| \tilde{\boldsymbol{f}}_i \|^2. \tag{52}$$

Since $\| \tilde{f}_i \|^2$ is still a random quantity, taking the expectation of Eq. 50 gives

$$\mathcal{E}\{\mathrm{SPE} - \mathrm{SPE}_{i|0}\} = \mathcal{E}\{\| \tilde{f}_i \|^2\} = \tilde{u}_i. \tag{53}$$

Therefore, the expected reduction in the SPE due to reconstruction in $\mathcal{S}_i$ is identical to $\tilde{u}_i$. This result can be used to estimate the confidence region for $\mathrm{SPE}_{i|0}$ when its probabilistic distribution is the same as that for SPE,

$$\delta_i^2 = \delta^2 - \tilde{u}_i. \tag{54}$$

The preceding relation assumes that reconstruction affects only the mean of the probabilistic distribution of SPE. An alternative way to estimate δ_i is by applying the same guidelines used for δ, for example, to define a threshold for the $\mathrm{SPE}_{i|0}$ using fault-free data. In many cases $\tilde{u}_i$ in Eq. 54 is small compared to δ^2. Hence, one can use δ^2 to approximate δ_i^2, which yields more reliable identification.

We consider the following possible scenarios for the identification of the actual fault.

$\mathcal{F}_i$ Occurs but $\mathcal{F}_j \neq \mathcal{F}_i$ Is Reconstructed. When $\mathcal{F}_i$ occurs and $\mathcal{F}_j \neq \mathcal{F}_i$ is assumed, the $\mathrm{SPE}_{j|i}$ in Eq. 47 becomes

$$\mathrm{SPE}_{j|i} = \tilde{x}^T \left(I - \tilde{\Xi}_j^\circ \Xi_j^{\circ T} \right) \tilde{x} = \mathrm{SPE} - \| \tilde{f}_j \|^2, \tag{55}$$

where Eq. 27 is used in the preceding relation. Note that the SPE in the preceding equation includes the actual fault magnitude. The larger the fault magnitude, the larger is SPE, and thus $\mathrm{SPE}_{j|i}$. Therefore, to sufficiently identify $\mathcal{F}_i$ from other possible candidates $\{\mathcal{F}_j\}$, that is, to make $\mathrm{SPE}_{j|i} > \delta_j^2$, it is desirable to have a large SPE and small $\| \tilde{f}_j \|^2$. The conditions required to identify $\mathcal{F}_i$ from $\{\mathcal{F}_j\}$ are derived in the next subsection.

The assumed fault $\mathcal{F}_j$ is the actual fault $\mathcal{F}_i$. In this case, the $\mathrm{SPE}_{i|i}$ is the same as $\mathrm{SPE}_{i|0}$, that is,

$$\mathrm{SPE}_{i|i} \leq \delta_i^2 \tag{56}$$

indicates that the actual fault is identified.

An important remark is that as long as $\mathcal{F}_i \in \{\mathcal{F}_j\}$, $\mathcal{F}_i$ can always be identified, which makes $\mathrm{SPE}_{i|i} \leq \delta_i^2 \leq \delta^2$. The only requirement is the feasibility to calculate $\tilde{f}_i$, that is, $\mathcal{F}_i$ is reconstructable. Nevertheless, if $\mathcal{F}_i$ is not reconstructable, it is also not detectable. Another remark is that it is possible to have $\mathrm{SPE}_{j|i} \leq \delta_i^2$, but $\mathcal{F}_j \neq \mathcal{F}_i$. In this case, $\mathcal{F}_j$ and $\mathcal{F}_i$ are not isolatable, making the unique identification of $\mathcal{F}_i$ impossible. However, we can find a subset of the fault from the entire set, which narrows down the possible candidates for the actual fault. Alternative approaches can be taken to further identify the actual fault. The conditions for identifiability will be derived in the next subsection.

Identification index

Dunia et al. (1996) have shown that the ratio $\mathrm{SPE}_j/\mathrm{SPE}$ is a well-defined index for fault identification, based on Eq. 55,

$$\eta_j^2 \equiv \frac{\mathrm{SPE}_j}{\mathrm{SPE}} = 1 - \frac{\| \tilde{f}_j \|^2}{\mathrm{SPE}}, \tag{57}$$

where $\eta_j \in [0, 1]$ represents the identification index for $\mathcal{F}_j$ (Dunia and Qin, 1998). The identification index can be defined for partial and complete reconstruction of faults. If $\mathcal{F}_i$ is the actual fault, $\eta_i^2 \to 0$. To illustrate this tendency we substitute Eq. 27 in Eq. 57,

$$\eta_i^2 = 1 - \frac{\| \tilde{\Xi}_i^{\circ T} \left(\tilde{x}^* + \tilde{\Xi}_i^\circ \tilde{f} \right) \|^2}{\| \tilde{x}^* + \tilde{\Xi}_i^\circ f \|^2} = 1 - \frac{\| \tilde{\Xi}_i^{\circ T} \tilde{x}^* + \tilde{f} \|^2}{\| \tilde{x}^* + \tilde{\Xi}_i^\circ \tilde{f} \|^2} \tag{58}$$

$$\to 1 - \frac{\| \tilde{f} \|^2}{\| \tilde{\Xi}_i^\circ \tilde{f} \|^2} = 0 \tag{59}$$

when $\| \tilde{f} \|$ is large or dominant. A confidence limit for the identification index can be defined based on δ_i,

$$\eta_i^2 \, \mathrm{SPE} = \mathrm{SPE}_i \leq \delta_i^2, \tag{60}$$

which makes the ratio δ_i^2/SPE an adjustable confidence limit for η_i^2.

Fault Isolatability

The fault identification task is concerned with identifying the actual fault $\mathcal{F}_i$ from the set $\{\mathcal{F}_j\}$. In our earlier work (Dunia and Qin, 1998), where unidimensional faults are considered, we used the identification index to identify the actual fault. If only one index among $\{\eta_j\}$ is close to zero, then the actual fault is uniquely identifiable. Otherwise, we may find a few candidates that bring η_i close to zero, making unique identification impossible.

Since the identification procedure assumes a candidate $\mathcal{F}_j$ for the actual fault $\mathcal{F}_i$, the identifiability of $\mathcal{F}_i$ from the set $\{\mathcal{F}_j\}$ is identical to the isolatability of two faults $\mathcal{F}_i$ and $\mathcal{F}_j (j = 1, 2, \ldots, J)$. Therefore, the identifiability and isolatability of two faults are interchangeable. We discuss the isolation of two faults and derive the isolatability conditions in this subsection.

Fault isolation

Fault isolation determines whether another fault $\mathcal{F}_j$ is also identified as the cause when $\mathcal{F}_i$ occurs. In other words, the assumption that $\mathcal{F}_j$ occurred should make $\mathrm{SPE}_{j|i}$ above the confidence limit when the fault $\mathcal{F}_i \neq \mathcal{F}_j$ is affecting the pro-

cess. In general, a fault $\mathcal{F}_j$ is rejected as the possible cause of the fault when

$$\mathrm{SPE}_{j|i} \equiv \| \tilde{\boldsymbol{x}}_j \|^2 > \delta_j^2. \tag{61}$$

The preceding condition makes $\mathcal{F}_i$ and $\mathcal{F}_j$ sufficiently isolatable. To achieve this condition, some necessary preconditions have to be in place.

(i) Fault $\mathcal{F}_i$ has to satisfy the necessary condition for detectability, that is, $\tilde{\boldsymbol{\Xi}}_i \boldsymbol{f} \neq \boldsymbol{0}$; otherwise SPE is not affected by $\mathcal{F}_i$.

(ii) Fault $\mathcal{F}_j$ has to be reconstructable, that is, $\tilde{\boldsymbol{\Xi}}_j \neq \boldsymbol{0}$.

Obviously if all faults are necessarily detectable, that is, $\{\tilde{\boldsymbol{\Xi}}_i \boldsymbol{f} \neq \boldsymbol{0},\ i = 1, 2, \ldots\}$, the preceding conditions are satisfied. In the subsequent discussion of isolatability, we assume the necessary detectability condition for all faults; otherwise, no abnormality is detected and thus no isolation.

We now examine the relation between the two fault subspaces: $\mathbb{S}_i$ and $\mathbb{S}_j$, which represent $\mathcal{F}_i$ and $\mathcal{F}_j$, respectively. We have the following four possible situations:

(a) $\tilde{\mathbb{S}}_i$ and $\tilde{\mathbb{S}}_j$ do not overlap, that is, $\tilde{\mathbb{S}}_i \cap \tilde{\mathbb{S}}_j = \boldsymbol{0}$.
(b) $\tilde{\mathbb{S}}_i$ and $\tilde{\mathbb{S}}_j$ partially overlap, that is, $\tilde{\mathbb{S}}_i \cap \mathbb{S}_j \neq \boldsymbol{0}$.
(c) $\tilde{\mathbb{S}}_j \subset \tilde{\mathbb{S}}_i$.
(d) $\tilde{\mathbb{S}}_i \subseteq \tilde{\mathbb{S}}_j$.

In case (a), the two faults may be *completely isolatable*, regardless of the direction of $\boldsymbol{f}$. In cases (b) and (c), the isolatability depends on the magnitude and direction of $\boldsymbol{f}$. Case (d) shows that $\mathcal{F}_i$ cannot be isolated from $\mathcal{F}_j$. Next we derive the necessary and sufficient conditions for complete isolatability and partial isolatability.

Complete isolatability

A fault $\mathcal{F}_i$ is completely isolatable from another fault $\mathcal{F}_j$ if there is no $\tilde{\boldsymbol{f}} \neq \boldsymbol{0}$ such that

$$\tilde{\boldsymbol{\Xi}}_i^{\circ} \tilde{\boldsymbol{f}} \in \Re\left\{\tilde{\boldsymbol{\Xi}}_j^{\circ}\right\}. \tag{62}$$

The preceding condition indicates that there is no nonzero common vector between $\tilde{\mathbb{S}}_i$ and $\tilde{\mathbb{S}}_j$. Therefore, $\tilde{\mathbb{S}}_i \cap \tilde{\mathbb{S}}_j = \boldsymbol{0}$ is a necessary condition to make $\mathcal{F}_i$ and $\mathcal{F}_j$ *completely isolatable*.

Another statement for complete isolatability is that the projection of $\tilde{\boldsymbol{\Xi}}_i^{\circ} \tilde{\boldsymbol{f}}$ onto $\mathbb{S}_j^{\perp}$ is not zero for all $\tilde{\boldsymbol{f}} \in \Re^{\tilde{l}_i}$, except for $\tilde{\boldsymbol{f}} = \boldsymbol{0}$. This condition indicates that none of the directions of $\tilde{\boldsymbol{\Xi}}_i^{\circ}$ vanish when projecting onto $\tilde{\mathbb{S}}_j^{\perp}$. Note that the columns of $\boldsymbol{I} - \tilde{\boldsymbol{\Xi}}_j^{\circ} \tilde{\boldsymbol{\Xi}}_j^{\circ T}$ spans $\tilde{\mathbb{S}}_j^{\perp}$. Therefore, it is necessary to verify if the matrix $(\boldsymbol{I} - \tilde{\boldsymbol{\Xi}}_j^{\circ} \tilde{\boldsymbol{\Xi}}_j^{\circ T}) \tilde{\boldsymbol{\Xi}}_i^{\circ}$ has full column rank. According to Eq. 48, $(\boldsymbol{I} - \tilde{\boldsymbol{\Xi}}_j^{\circ} \tilde{\boldsymbol{\Xi}}_j^{\circ T}) \tilde{\boldsymbol{\Xi}}_i^{\circ}$ having full column rank necessarily increases $\mathrm{SPE}_{j|i}$ for any $\tilde{\boldsymbol{f}} \neq \boldsymbol{0}$. In summary, one of the following statements is necessary to determine if $\boldsymbol{F}_i$ is completely isolatable from $\mathcal{F}_j$.

(i) $\tilde{\mathbb{S}}_i \cap \tilde{\mathbb{S}}_j = \boldsymbol{0}$.
(ii) $\boldsymbol{I} - \tilde{\boldsymbol{\Xi}}_i^{\circ T} \tilde{\boldsymbol{\Xi}}_j^{\circ} \tilde{\boldsymbol{\Xi}}_i^{\circ}$ is full rank.
(iii) $(\boldsymbol{I} - \tilde{\boldsymbol{\Xi}}_j^{\circ} \tilde{\boldsymbol{\Xi}}_j^{\circ T})\, \tilde{\boldsymbol{\Xi}}_i^{\circ}$ has full column rank.
(iv) $\sigma_{\min}\{(\boldsymbol{I} - \tilde{\boldsymbol{\Xi}}_j^{\circ} \tilde{\boldsymbol{\Xi}}_j^{\circ T}) \tilde{\boldsymbol{\Xi}}_i^{\circ}\} > 0$.

Note that the condition for complete isolatability between faults is reciprocal; if $\mathcal{F}_i$ is completely isolatable from $\mathcal{F}_j$, $\mathcal{F}_j$ is also completely isolatable from $\mathcal{F}_i$. This is shown simply by statement (i).

Finally, to guarantee that $\mathrm{SPE}_{j|i}$ will always be greater than δ_j^2 when $\mathcal{F}_i$ has occurred, the fault magnitude has to be large enough, which gives the sufficient condition for isolatability. To obtain the sufficient condition for isolatability, we require $\mathrm{SPE}_{j|i} > \delta^2$, which guarantees $\mathrm{SPE}_{j|i} > \delta_i^2$. Since $\tilde{\boldsymbol{x}}^*$ is a random vector and represents the normal situation, we minimize $\mathrm{SPE}_{j|i}$ with respect to $\tilde{\boldsymbol{x}}^*$, subject to $\| \tilde{\boldsymbol{x}}^* \| \leq \delta$,

$$\min_{\| \tilde{\boldsymbol{x}}^* \| \leq \delta} \mathrm{SPE}_{j|i}. \tag{63}$$

Appendix B shows that the solution of Eq. 63 is given by

$$\tilde{\boldsymbol{x}}^* = \frac{\pm \delta \left(\boldsymbol{I} - \tilde{\boldsymbol{\Xi}}_j^{\circ} \tilde{\boldsymbol{\Xi}}_j^{\circ T}\right) \tilde{\boldsymbol{\Xi}}_i^{\circ} \tilde{\boldsymbol{f}}}{\| \left(\boldsymbol{I} - \tilde{\boldsymbol{\Xi}}_j^{\circ} \tilde{\boldsymbol{\Xi}}_j^{\circ T}\right) \tilde{\boldsymbol{\Xi}}_i^{\circ} \tilde{\boldsymbol{f}} \|}, \tag{64}$$

which is the worst $\tilde{\boldsymbol{x}}^*$ for $\mathrm{SPE}_{j|i}$, and Eq. 48 leads to

$$\| \left(\boldsymbol{I} - \tilde{\boldsymbol{\Xi}}_j^{\circ} \tilde{\boldsymbol{\Xi}}_j^{\circ T}\right) \tilde{\boldsymbol{\Xi}}_i^{\circ} \tilde{\boldsymbol{f}} \| > 2\delta. \tag{65}$$

The following remarks are made in reference to these expressions:

(i) The condition provided by Eq. 65 implies sufficient detectability because

$$\| \tilde{\boldsymbol{f}} \| \geq \| \left(\boldsymbol{I} - \tilde{\boldsymbol{\Xi}}_j^{\circ} \tilde{\boldsymbol{\Xi}}_j^{\circ T}\right) \tilde{\boldsymbol{\Xi}}_i^{\circ} \tilde{\boldsymbol{f}} \| > 2\delta.$$

(ii) In the case of $\tilde{\mathbb{S}}_i \perp \tilde{\mathbb{S}}_j$, the sufficient condition for isolatability would be given by

$$\| \left(\boldsymbol{I} - \tilde{\boldsymbol{\Xi}}_j^{\circ} \tilde{\boldsymbol{\Xi}}_j^{\circ T}\right) \tilde{\boldsymbol{\Xi}}_i^{\circ} \tilde{\boldsymbol{f}} \| = \| \boldsymbol{f} \| > 2\delta,$$

which is equivalent to the sufficient condition for detectability.

(iii) Since

$$\| \left(\boldsymbol{I} - \tilde{\boldsymbol{\Xi}}_j^{\circ} \tilde{\boldsymbol{\Xi}}_j^{\circ T}\right) \tilde{\boldsymbol{\Xi}}_i^{\circ} \tilde{\boldsymbol{f}} \|^2 \geq \sigma_{\min}^2 \left\{ \left(\boldsymbol{I} - \tilde{\boldsymbol{\Xi}}_j^{\circ} \tilde{\boldsymbol{\Xi}}_j^{\circ T}\right) \tilde{\boldsymbol{\Xi}}_i^{\circ} \right\} \| \tilde{\boldsymbol{f}} \|^2,$$

the following relation guarantees sufficient isolatability,

$$\| \tilde{\boldsymbol{f}} \| > \frac{2\delta}{\sigma_{\min} \left\{ \left(\boldsymbol{I} - \tilde{\boldsymbol{\Xi}}_j^{\circ} \tilde{\boldsymbol{\Xi}}_j^{\circ T}\right) \tilde{\boldsymbol{\Xi}}_i^{\circ} \right\}},$$

where $\sigma_{\min}\{(\boldsymbol{I} - \tilde{\boldsymbol{\Xi}}_j^{\circ} \tilde{\boldsymbol{\Xi}}_j^{\circ T}) \tilde{\boldsymbol{\Xi}}_i^{\circ}\} > 0$ is the minimum singular value of $(\boldsymbol{I} - \tilde{\boldsymbol{\Xi}}_j^{\circ} \tilde{\boldsymbol{\Xi}}_j^{\circ T}) \tilde{\boldsymbol{\Xi}}_i^{\circ}$.

Partial isolatability

It is possible that the $\tilde{\mathbb{S}}_i \cap \tilde{\mathbb{S}}_j \neq \mathbf{0}$, where complete isolation is not possible. In this case, $\sigma_{min}\{(\boldsymbol{I} - \tilde{\boldsymbol{\Xi}}_j^{\circ}\tilde{\boldsymbol{\Xi}}_j^{\circ T})\tilde{\boldsymbol{\Xi}}_i^{\circ}\} = 0$. However, partial isolation is still possible, depending on $\tilde{f}$. A necessary condition to satisfy Eq. 61 via Eq. 48 requires

$$\left(\boldsymbol{I} - \tilde{\boldsymbol{\Xi}}_j^{\circ}\tilde{\boldsymbol{\Xi}}_j^{\circ T}\right)\tilde{\boldsymbol{\Xi}}_i^{\circ}\tilde{f} \neq \mathbf{0}, \tag{66}$$

which implies

$$\tilde{\boldsymbol{\Xi}}_i^{\circ T}\tilde{\boldsymbol{\Xi}}_j^{\circ}\tilde{\boldsymbol{\Xi}}_j^{\circ T}\tilde{\boldsymbol{\Xi}}_i^{\circ} \neq \boldsymbol{I} \tag{67}$$

and

$$\tilde{\boldsymbol{\Xi}}_i^{\circ}\tilde{f} \neq \mathbf{0} \tag{68}$$

The lefthand side of Eq. 67 has been used by Krzanowski (1979) to compare the eigenvectors of two matrices, and by McBrayer (1995) to determine the similarity between fault models based on bias terms in process variables. This work provides the conditions for the basis and magnitude of a fault to isolate it from other faults.

We notice that the eigenvalues of $\boldsymbol{I} - \tilde{\boldsymbol{\Xi}}_j^{\circ}\tilde{\boldsymbol{\Xi}}_j^{\circ T}$ are either zero or one, and the eigenvectors of zero eigenvalues are the columns of $\tilde{\boldsymbol{\Xi}}_j^{\circ}$. Therefore, to satisfy Eq. 66 we need to assure that

$$\mathcal{R}\{\tilde{\boldsymbol{\Xi}}_i^{\circ}\} \not\subseteq \mathcal{R}\left\{\tilde{\boldsymbol{\Xi}}_j^{\circ}\right\}$$

or

$$\tilde{\mathbb{S}}_i \not\subseteq \tilde{\mathbb{S}}_j.$$

We summarize the necessary conditions for partial isolatability of $\mathcal{F}_i$ and $\mathcal{F}_j$ as follows:

(a) If $\mathcal{F}_i$ is (partially) isolatable from $\mathcal{F}_j$, one of the following conditions is true:

(i) $\mathbb{S}_i \not\subseteq \mathbb{S}_j$

(ii) $\tilde{\boldsymbol{\Xi}}_i^{\circ T}\tilde{\boldsymbol{\Xi}}_j^{\circ}\tilde{\boldsymbol{\Xi}}_j^{\circ T}\tilde{\boldsymbol{\Xi}}_i^{\circ} \neq \mathbf{I}$

(iii) $\left(\boldsymbol{I} - \tilde{\boldsymbol{\Xi}}_j^{\circ}\tilde{\boldsymbol{\Xi}}_j^{\circ T}\right)\tilde{\boldsymbol{\Xi}}_i^{\circ} \neq \mathbf{0}$, or

(iv) $\sigma_{\max}\left\{\left(\boldsymbol{I} - \tilde{\boldsymbol{\Xi}}_j^{\circ}\tilde{\boldsymbol{\Xi}}_j^{\circ T}\right)\tilde{\boldsymbol{\Xi}}_i^{\circ}\right\} > 0.$

(b) $\mathcal{F}_i$ is not isolatable from $\mathcal{F}_j$ if $(\boldsymbol{I} - \tilde{\boldsymbol{\Xi}}_j^{\circ}\tilde{\boldsymbol{\Xi}}_j^{\circ T})\tilde{\boldsymbol{\Xi}}_i^{\circ}\tilde{f} = \mathbf{0}$, even though $\mathcal{F}_i$ may be detectable.

Although the necessary condition for partial isolatability is satisfied, the magnitude of $\tilde{f}$ has to be large enough to make $\mathcal{F}_i$ sufficiently isolatable from $\mathcal{F}_j$, that is,

$$\mathrm{SPE}_{j|i} > \delta^2. \tag{69}$$

Similar to the derivation for complete isolation, the minimum $\mathrm{SPE}_{j|i}$ is given by

$$\tilde{x}^* = \frac{\pm\,\delta\left(\boldsymbol{I} - \tilde{\boldsymbol{\Xi}}_j^{\circ}\tilde{\boldsymbol{\Xi}}_j^{\circ T}\right)\tilde{\boldsymbol{\Xi}}_i^{\circ}\tilde{f}}{\left\|\left(\boldsymbol{I} - \tilde{\boldsymbol{\Xi}}_j^{\circ}\tilde{\boldsymbol{\Xi}}_j^{\circ T}\right)\tilde{\boldsymbol{\Xi}}_i^{\circ}\tilde{f}\right\|}. \tag{70}$$

This representation is feasible because of the necessary condition for partial isolatability. Similarly, to make $\mathrm{SPE}_{j|i} > \delta^2$, we must require

$$\left\|\left(\boldsymbol{I} - \tilde{\boldsymbol{\Xi}}_j^{\circ}\tilde{\boldsymbol{\Xi}}_j^{\circ T}\right)\tilde{\boldsymbol{\Xi}}_i^{\circ}\tilde{f}\right\| > 2\delta. \tag{71}$$

Equation 71 provides the sufficient condition for partial isolatability.

It should be noted that, although the partial isolatability and complete isolatability are fundamentally different, we can consider the complete isolatability as a special case for partial isolatability. Therefore, we can perform SVD for $(\boldsymbol{I} - \tilde{\boldsymbol{\Xi}}_j^{\circ}\tilde{\boldsymbol{\Xi}}_j^{\circ T})\tilde{\boldsymbol{\Xi}}_i^{\circ}$. If all singular values are larger than zero, $\mathcal{F}_i$ is completely isolatable from $\mathcal{F}_j$; if some of the singular vales of $(\boldsymbol{I} - \tilde{\boldsymbol{\Xi}}_j^{\circ}\tilde{\boldsymbol{\Xi}}_j^{\circ T})\tilde{\boldsymbol{\Xi}}_i^{\circ}$ are zero and $\tilde{f} \not\subseteq \mathcal{U}\{(\boldsymbol{I} - \tilde{\boldsymbol{\Xi}}_j^{\circ}\tilde{\boldsymbol{\Xi}}_j^{\circ T})\tilde{\boldsymbol{\Xi}}_i^{\circ}\}$, $\mathcal{F}_i$ is partially isolatable from $\mathcal{F}_j$; otherwise, $\mathcal{F}_i$ is not isolatable from $\mathcal{F}_j$. To guarantee isolatability, Eq. 71 has to be satisfied.

Figure 6 illustrates the partial and complete isolatability of fault $\mathcal{F}_i$ from fault $\mathcal{F}_j$. Note that only the projections of $\mathbb{S}_j$ and $\mathbb{S}_i$ to $\tilde{\mathbb{S}}$ are considered to determine isolatability because these projections are used to calculate the SPE_i and $\mathrm{SPE}_{j|i}$, respectively. In the top portion of the figure, the intersection of $\tilde{\mathbb{S}}_i$ and $\tilde{\mathbb{S}}_j$ is not $\mathbf{0}$, which provides abnormal conditions described by both subspace basis. However, if $\tilde{\mathbb{S}}_j \cap \tilde{\mathbb{S}}_i = \mathbf{0}$ (bottom), the faults are completely isolatable because no abnormal condition belongs to both subspaces. Note that the conditions for partial isolatability of $\mathcal{F}_i$ from $\mathcal{F}_j$ are not reciprocal. Figure 7 illustrates the situation where $\mathcal{F}_j$ is partially isolatable from $\mathcal{F}_i$, but $\mathcal{F}_i$ is not isolatable from $\mathcal{F}_j$.

The complete procedure of the proposed method for fault identification and reconstruction can be summarized as follows:

1. Obtain normal process data and fault direction vectors or matrices for each process or sensor fault.
2. Build PCA models using various numbers of PCs. Determine whether all faults detectable and reconstructable by examining the singular values of $\{\tilde{\boldsymbol{\Xi}}_i\}$. Remove faults that fail to meet the necessary condition of detectability and reconstructability.
3. Build a refined PCA model with properly selected sensors and number of PCs using the procedure given in the section on inclusion of faults and variables of this article. Only fault direction vectors or matrices are required in this step; these faults need not actually occur to accomplish this step.
4. Determine whether fault $\boldsymbol{\Xi}_i$ is isolatable from fault $\boldsymbol{\Xi}_j$ by examining the singular values of $(\boldsymbol{I} - \tilde{\boldsymbol{\Xi}}_j^{\circ}\tilde{\boldsymbol{\Xi}}_j^{\circ T})\tilde{\boldsymbol{\Xi}}_i^{\circ}$.
5. Perform on-line fault detection, identification, and reconstruction. Fault identification is performed by monitoring the identification index defined in Eq. 57.

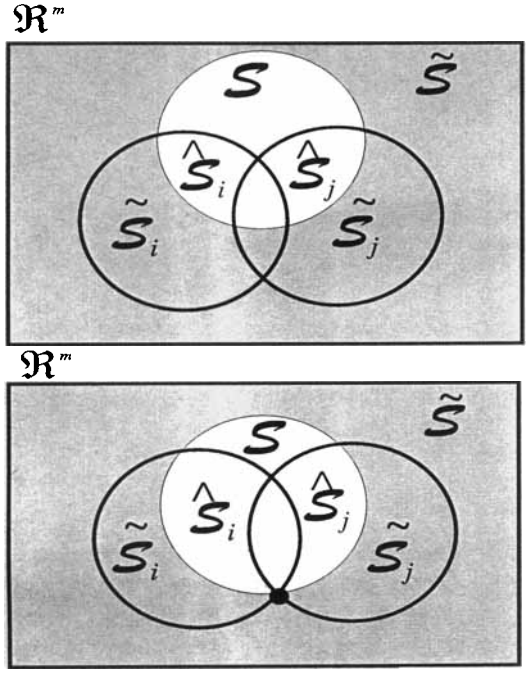

Figure 6. Partial and complete isolatability of $\mathfrak{F}_i$ from $\mathfrak{F}_j$.

For the case of $\tilde{\mathbb{S}}_j \cap \tilde{\mathbb{S}}_i \neq \mathbf{0}$ (top), both faults are potential causes of an abnormal condition. However, for $\tilde{\mathbb{S}}_j \cap \tilde{\mathbb{S}}_i = \mathbf{0}$ (bottom), the faults are completely isolatable.

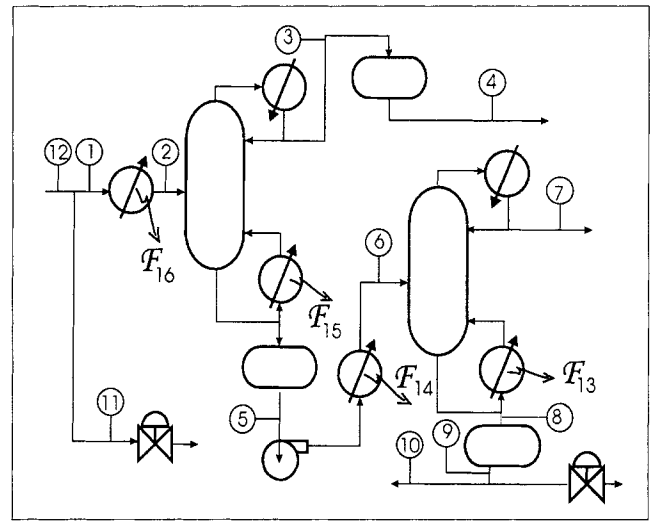

Figure 8. Simulated process.

Twelve sensor faults are considered. Leaks at the preheaters and reboilers are process faults $\mathfrak{F}_{13}$, $\mathfrak{F}_{14}$, $\mathfrak{F}_{15}$, and $\mathfrak{F}_{16}$.

Case Study for a Simulated Process

Consider the process flow diagram of Figure 8. Two separation columns are used to obtain three different products. The bottom of the first column is taken to the second column to obtain a second stream of light products. The control valves and the columns distribute the material flow, depending on the feedstock composition and production needs. A total of 12 flow measurements are taken along the process. We consider all the sensor faults and leaks at each reboiler and preheater. The first 12 faults correspond to the unidimensional sensor faults, which are characterized by the following directions:

$$[\Xi_1 \quad \Xi_2 \ldots \Xi_{11} \quad \Xi_{12}] = \boldsymbol{I},$$

where the Ξ_is are column vectors; and the last four faults correspond to the leaks at the reboilers ($\mathfrak{F}_{13}$ and $\mathfrak{F}_{15}$) and preheaters ($\mathfrak{F}_{14}$ and $\mathfrak{F}_{16}$). Appendix C shows how these fault descriptions are obtained and transformed for the use of this algorithm. A total of 1,000 samples were generated randomly for the calculation of the correlation matrix at normal process conditions.

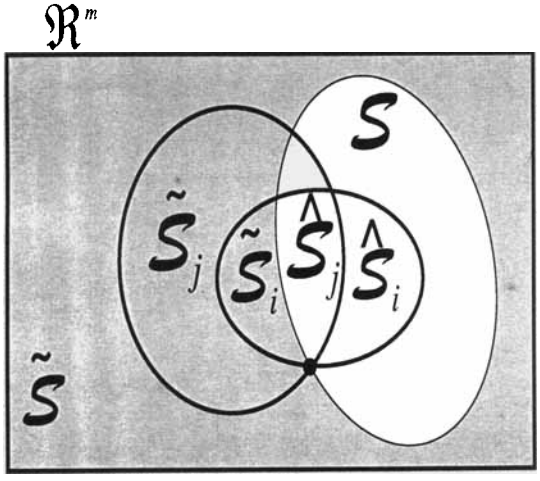

Figure 7. Fault $\mathfrak{F}_i$ cannot be isolated from fault $\mathfrak{F}_j$ because $\tilde{\mathbb{S}}_i \subset \tilde{\mathbb{S}}_j$.

Note that both faults are partially reconstructed because the intersection of $\mathbb{S}_i$ and $\mathbb{S}_j$ with $\mathbb{S}$ is not the null vector, ●.

Detectability and reconstructability

Detectability and reconstructability of the faults are verified by testing whether or not $\tilde{\boldsymbol{\Xi}}_i$ is $\mathbf{0}$, which is easily verified by examining whether or not $\sigma_{\max}\{\tilde{\boldsymbol{\Xi}}_i\} = 0$. It turns out that all faults are detectable and at least partially reconstructable.

To determine whether all faults are *reliably* reconstructable, that is, $u_i < \varrho_i$, the procedure given in the fourth section is used by (1) dropping out sensors that are not correlated; (2) dropping out insignificant singular values of $\tilde{\boldsymbol{\Xi}}_i$ to reduce u_i; and (3) dropping out process faults that are not reliably reconstructed. Whenever a principal component is included in the model or a sensor is dropped out, $\sigma_{\max}\{\tilde{\boldsymbol{\Xi}}_i\}$ changes. Table 1 shows the maximum singular value, $\sigma_{\max}\{\tilde{\boldsymbol{\Xi}}_i\}$, for all sensor faults and $l \in [1, 5]$. Note that for $l \in [1, 4]$ all sensors are reliably reconstructed; therefore, no sensors are deleted. However, $l = 5$, sensor 2 could not be *reliably* reconstructed and would be dropped out if the final model requires more than four PCs. If this is the case, sensor 2 would be better monitored using a univariate approach rather than the PCA-based approach. However, if the final PCA model

Table 1. Maximum Singular Value of $\tilde{\Xi}_i$ for Different Number of Principal Components*

	l				
i	1	2	3	4	5
1	0.94	0.91	0.91	0.91	0.64
2	0.98	0.83	0.82	0.80	N/A
3	0.94	0.92	0.92	0.91	0.75
4	0.98	0.82	0.81	0.79	0.75
5	0.93	0.92	0.92	0.89	0.87
6	0.93	0.93	0.92	0.88	0.87
7	0.96	0.96	0.96	0.70	0.65
8	0.95	0.91	0.91	0.84	0.81
9	0.94	0.90	0.90	0.84	0.79
10	0.95	0.91	0.91	0.84	0.58
11	1.00	1.00	0.55	0.55	0.54
12	0.96	0.94	0.79	0.79	0.78
13	1.00	1.00	1.00	1.00	0.73
14	1.00	1.00	1.00	1.00	0.74
15	1.00	1.00	0.94	0.91	0.79
16	1.00	1.00	0.86	0.86	0.71

*Although the singular value decreases with l, it is different than zero, making the faults detectable and reconstructable in the range shown later in the text. Although the faults are reconstructable, reconstruction is not always reliable when some faults are assumed, like in the case of $\mathfrak{F}_2$ when using $l = 5$.

Table 3. Unreconstructed Variance as a Function of l.*

		l					
i	$\tilde{l}_i$	1	2	3	4	5	6
1	1	0.47	0.36	0.36	0.35	0.64	N/A
2	1	0.87	0.44	0.41	0.35	N/A	N/A
3	1	0.46	0.38	0.38	0.37	0.38	N/A
4	1	0.89	0.46	0.42	0.35	0.38	N/A
5	1	0.37	0.31	0.31	0.24	0.25	N/A
6	1	0.37	0.30	0.30	0.22	0.22	N/A
7	1	0.72	0.72	0.72	0.31	0.32	N/A
8	1	0.54	0.40	0.40	0.23	0.23	N/A
9	1	0.53	0.37	0.37	0.23	0.24	N/A
10	1	0.63	0.50	0.50	0.39	0.80	N/A
11	1	1.00	1.00	0.85	0.79	0.81	N/A
12	1	0.69	0.63	0.38	0.38	0.39	N/A
13	2	2.22	2.33	2.34	1.50	2.02	N/A
14	3	3.45	2.71	2.71	0.78(2)	1.17(2)	N/A
15	3	4.64	1.66(2)	0.37(1)	0.31(1)	0.39(1)	N/A
16	2	1.91	1.72	0.37(1)	0.36(1)	0.49(1)	N/A
	$q^T u$	10.66	8.72	7.57	**5.69**	6.77	—

*The minimum $q^T u$ is reached at $l = 4$. At $l = 5$ the second sensor is not reliably reconstructed because $u_2 > e_2$. The numbers in parenthesis represent the dimension of $\mathbb{S}_i$ in the cases where $\mathfrak{F}_i$ is partially reconstructed. In the case of $l = 6$, the model overfits the data and all the sensors/sensor faults are dropped out.

requires less than five principal components, sensor 2 can be reliably reconstructed.

To check the condition for complete reconstruction of the multidimensional faults $\mathfrak{F}_{13}$ through $\mathfrak{F}_{16}$, we check whether or not $\sigma_{\min}\{\tilde{\Xi}_i\} = 0$. Table 2 shows that these singular values are not zero, which indicates that all faults are completely reconstructable. However, we still need to check whether all reconstructions are *reliable*, that is, whether $u_i < \varrho_i$, which is shown later.

Selecting the number of principal components

The minimization of $q^T u$ will determine the optimal number of principal components for fault reconstruction. We consider that all the faults have the same importance in reconstruction. Because u_i increases with the dimension of the fault subspace, which tends to give more importance to the faults with larger subspace dimensions, the elements of q are set to $1/\varrho_i$. In this way q normalizes the unreconstructed variances with respect to their limits, ϱ_i, which takes into account the subspace dimension.

Table 3 provides u_i for $l = 1$ to 6. Note that this table can be calculated based on the PCA model and fault directions only; there is no need to generate or simulate these faults since the unreconstructed variance is independent of the fault magnitudes. The columns for l from 1 through 4 are generated with all sensors since they are reliably reconstructed. The column for $l = 5$ is generated after deleting sensor 2, since its unreconstructed variance is larger than its variance. The following remarks are made from the results of this table.

- The numbers in parentheses represent the dimensions of $\mathbb{S}_i$ required for reliable reconstruction. These faults were partially reconstructed because u_i would be larger than ϱ_i if completely reconstructed and some directions were dropped out to satisfy $u_i \le \varrho_i$.
- The multivariable faults $\mathfrak{F}_{13}$ to $\mathfrak{F}_{16}$ after dropping dimensions in $\mathbb{S}_i$ indeed have reduced unreconstructed variance.
- The minimum $q^T u = 5.7$ occurs at $l = 4$, where faults $\mathfrak{F}_{14}$ to $\mathfrak{F}_{16}$ are partially reconstructed.
- Sensor 2 would have been dropped out if $l = 5$ is optimal. Fortunately, it is kept in the model since the optimal l is 4.
- In the case of $l = 6$, the model overfits the data and none of the variables can be reliably reconstructed.

Figure 9 illustrates the weighted sum of unreconstructed variance and its projection onto $\mathbb{S}$ and $\tilde{\mathbb{S}}$, given by $q^T\hat{u}$ and $q^T\tilde{u}$, respectively. As is indicated earlier in the article, the latter is monotonically decreasing with l, while the former tends to increase with l. The sum of the two portions has a minimum at $l = 4$.

Fault isolatability. To determine if the set of faults is isolatable when using the optimal model, we examine if $\sigma_{\max}\{(I - \tilde{\Xi}_j^{\circ}\tilde{\Xi}_j^{\circ T})\tilde{\Xi}_i^{\circ}\} \neq 0$ for each pair of reconstructable faults. Table 4 gives the values for $\sigma_{\max}\{(I - \tilde{\Xi}_j^{\circ}\tilde{\Xi}_j^{\circ T})\tilde{\Xi}_i^{\circ}\}$ for each pair of faults. Note that the table is not necessarily symmetric because the partial isolatability condition is not reciprocal. We observe that every pair of faults is isolatable except for the following cases:

Table 2. Minimum Singular Value of Ξ_i for Different Number of Principal Components.*

	l				
i	1	2	3	4	5
13	0.92	0.83	0.82	0.59	0.57
14	0.85	0.73	0.73	0.24	0.20
15	0.89	0.44	0.36	0.17	0.14
16	0.95	0.92	0.44	0.40	0.37

*The results for unidimensional faults ($\mathfrak{F}_1$ to $\mathfrak{F}_{12}$) can be taken from Table 1.

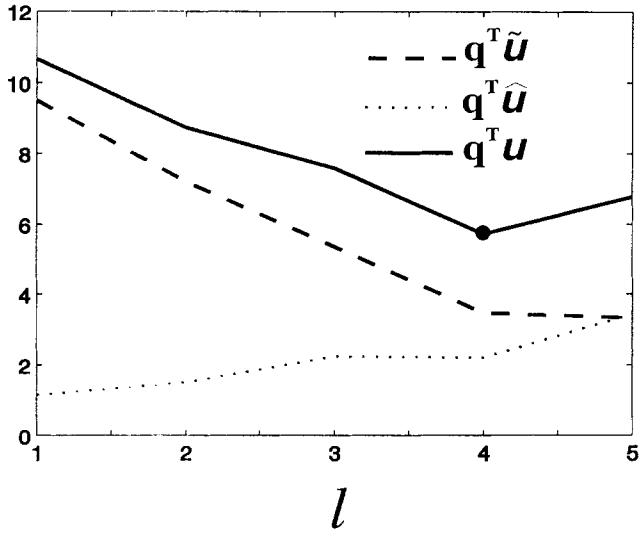

Figure 9. Effect of the number of principal components in the unreconstructed variance.

The projections $q^T\hat{u}$ and $q^T\tilde{u}$ are monotonically increasing and decreasing, respectively. The minimum for $q^T u = q^T\hat{u} + q^T\tilde{u}$ is achieved at $l = 4$.

- $\mathcal{F}_{11}$ from $\mathcal{F}_{12}$, and vice versa.
- $\mathcal{F}_{10}$ from $\mathcal{F}_{13}$ and $\mathcal{F}_{14}$.
- $\mathcal{F}_{7}$ from $\mathcal{F}_{13}$.

If $\sigma_{\min}\{(I - \tilde{\Xi}_j^{\circ}\tilde{\Xi}_j^{\circ T})\tilde{\Xi}_i^{\circ}\} \approx 0$, the faults are not completely isolatable. Table 5 depicts the minimum singular values $\sigma_{\min}\{(I - \tilde{\Xi}_j^{\circ}\tilde{\Xi}_j^{\circ T})\tilde{\Xi}_i^{\circ}\}$ for multidimensional faults. It is observed that, in addition to the nonisolatable faults just listed, the faults $\mathcal{F}_{13}$ and $\mathcal{F}_{14}$ are not completely isolatable. This result is expected because $\mathcal{F}_{13}$ and $\mathcal{F}_{14}$ overlap and share the subspace $\mathcal{S}_{10}$.

Conclusions and Discussion

Multidimensional fault detection, identification and reconstruction are proposed using a subspace approach. This approach can describe process faults using the concept of fault subspaces. The magnitude of the fault is provided by the coefficients used to represent the fault displacement that conforms to the subspace basis. This representation allows one to describe process and sensor faults from a multidimensional perspective, which generalizes the unidimensional approach used by Dunia and Qin (1998).

The multidimensional fault case considers the fault displacement from the location of the normal sample vector on the subspace that describes the fault. The normal sample vector satisfies the correlation imposed by the normal operation of the process. The correlation is captured in the PCA model, which partitions the measurement space into the PCS, where the process variations are according to the normal operation of the process, and the residual subspace, where the measurements deviate from the usual behavior of the process.

Necessary and sufficient conditions for fault detectability are developed based on the model basis, fault direction, and magnitude of the fault. These conditions depend on the discrepancy between the model subspace $\mathcal{S}$ and the fault subspace $\mathcal{S}_i$; the larger this discrepancy, the easier it is to detect the fault. It is shown in this work that this discrepancy is given by the projection of the fault basis on $\tilde{\mathbf{S}}$. If this projection is null, the fault is not detectable and any fault displacement will be considered as a normal variation of the process.

Reconstructability is defined in terms of the feasibility to estimate the normal sample vector in the presence of a fault. This property depends on the fault directions or subspace. The fault displacement that happened in the PCS only cannot be reconstructed. In the case that the fault subspace ($\mathcal{S}_i$) overlaps with $\mathcal{S}$, the fault can only be partially reconstructed. Necessary and sufficient conditions for partial and complete reconstruction are also developed in this work.

The concept of unreconstructed variance is extended in this article to the multidimensional fault case. The unreconstructed variance allows one to design the PCA model for best reconstruction. The unreconstructed variance for multidimensional faults represents a summation of variances in all the reconstructable directions of $\mathcal{S}_i$. Because some directions of $\mathcal{S}_i$ do not provide a reliable reconstruction of the fault $\mathcal{F}_i$,

Table 4. Maximum Singular Value of $(I - \tilde{\Xi}_j^{\circ}\tilde{\Xi}_j^{\circ T})\tilde{\Xi}_i^{\circ}$ for the Faults Descriptions and Optimum Model Obtained in the Example.*

i/j	1	2	3	4	5	6	7	8	9	10	11	12	13	14	15	16
1	·	0.98	0.97	0.97	0.99	0.99	0.98	1.00	1.00	1.00	0.99	0.99	0.99	0.96	0.85	0.64
2	0.98	·	0.98	0.98	0.99	0.99	0.98	1.00	1.00	1.00	0.99	0.99	0.99	0.95	0.86	0.96
3	0.97	0.98	·	0.81	1.00	0.99	0.98	1.00	1.00	1.00	0.99	0.98	0.99	0.97	0.89	0.95
4	0.97	0.98	0.81	·	0.99	0.99	0.98	1.00	1.00	1.00	0.98	0.99	0.99	0.96	0.89	0.95
5	0.99	0.99	1.00	0.99	·	0.96	0.91	0.99	0.99	0.99	1.00	1.00	0.89	0.78	0.97	0.99
6	0.99	0.99	0.99	0.99	0.96	·	0.91	0.99	0.99	1.00	1.00	1.00	0.89	0.70	0.97	0.99
7	0.98	0.98	0.98	0.98	0.91	0.91	·	0.97	0.98	0.97	1.00	1.00	0.15	0.90	0.92	0.97
8	1.00	1.00	1.00	1.00	0.99	0.99	0.97	·	0.91	0.91	1.00	1.00	0.85	0.91	1.00	1.00
9	1.00	1.00	1.00	1.00	0.99	0.99	0.98	0.91	·	0.91	1.00	1.00	0.84	0.91	1.00	1.00
10	1.00	1.00	1.00	1.00	0.99	1.00	0.97	0.91	0.91	·	1.00	1.00	0.00	0.04	1.00	1.00
11	0.99	0.99	0.99	0.98	1.00	1.00	1.00	1.00	1.00	1.00	·	0.07	0.99	0.98	0.92	0.83
12	0.99	0.99	0.98	0.99	1.00	1.00	1.00	1.00	1.00	1.00	0.07	·	0.99	0.99	0.93	0.86
13	1.00	1.00	1.00	1.00	1.00	1.00	1.00	1.00	1.00	1.00	1.00	1.00	·	0.95	1.00	1.00
14	1.00	1.00	1.00	1.00	1.00	1.00	1.00	1.00	1.00	1.00	1.00	1.00	0.95	·	1.00	1.00
15	0.85	0.86	0.89	0.89	0.97	0.97	0.92	1.00	1.00	1.00	0.92	0.93	0.96	0.84	·	0.72
16	0.64	0.96	0.95	0.95	0.99	0.99	0.97	1.00	1.00	1.00	0.83	0.86	0.98	0.94	0.72	·

*A singular value close to zero indicates that the fault i is not isolatable from fault j.

Table 5. Minimum Singular Value of $(I - \bar{\Xi}_j^{\circ}\bar{\Xi}_j^{\circ T})\bar{\Xi}_i^{\circ}$ for the Faults Descriptions and Optimum Model Obtained in the Example.*

i/j	1	2	3	4	5	6	7	8	9	10	11	12	13	14	15	16
1	·	0.98	0.97	0.97	0.99	0.99	0.98	1.00	1.00	1.00	0.99	0.99	0.99	0.96	0.85	0.64
2	0.98	·	0.98	0.98	0.99	0.99	0.98	1.00	1.00	1.00	0.99	0.99	0.99	0.95	0.86	0.96
3	0.97	0.98	·	0.81	1.00	0.99	0.98	1.00	1.00	1.00	0.99	0.98	0.99	0.97	0.89	0.95
4	0.97	0.98	0.81	·	0.99	0.99	0.98	1.00	1.00	1.00	0.98	0.99	0.99	0.96	0.89	0.95
5	0.99	0.99	1.00	0.99	·	0.96	0.91	0.99	0.99	0.99	1.00	1.00	0.89	0.78	0.97	0.99
6	0.99	0.99	0.99	0.99	0.96	·	0.91	0.99	0.99	1.00	1.00	1.00	0.89	0.70	0.97	0.99
7	0.98	0.98	0.98	0.98	0.91	0.91	·	0.97	0.98	0.97	1.00	1.00	0.15	0.90	0.92	0.97
8	1.00	1.00	1.00	1.00	0.99	0.99	0.97	·	0.91	0.91	1.00	1.00	0.85	0.91	1.00	1.00
9	1.00	1.00	1.00	1.00	0.99	0.99	0.98	0.91	·	0.91	1.00	1.00	0.84	0.91	1.00	1.00
10	1.00	1.00	1.00	1.00	0.99	1.00	0.97	0.91	0.91	·	1.00	1.00	0.00	0.04	1.00	1.00
11	0.99	0.99	0.99	0.98	1.00	1.00	1.00	1.00	1.00	1.00	·	0.07	0.99	0.98	0.92	0.83
12	0.99	0.99	0.98	0.99	1.00	1.00	1.00	1.00	1.00	1.00	0.07	·	0.99	0.99	0.93	0.86
13	0.99	0.99	0.99	0.99	0.89	0.89	0.15	0.85	0.84	0.00	0.99	0.99	·	0.03	0.96	0.98
14	0.96	0.95	0.97	0.96	0.78	0.70	0.90	0.91	0.91	0.04	0.98	0.99	0.03	·	0.84	0.94
15	0.85	0.86	0.89	0.89	0.97	0.97	0.92	1.00	1.00	1.00	0.92	0.93	0.96	0.84	·	0.72
16	0.64	0.96	0.95	0.95	0.95	0.99	0.97	1.00	1.00	1.00	0.83	0.86	0.98	0.94	0.72	·

*A singular value close to zero indicates that the faults i and j are not completely isolatable.

the dimension of $\mathbb{S}_i$ can be reduced to consider only the directions with reliable reconstruction. As a result, not only can we determine the number of principal components and sensors to use for monitoring, but also the dimension of the fault subspace for reliable reconstruction.

Fault identification is made via fault reconstruction. After a fault is detected, it is important to verify if another fault is also identified as the cause of the abnormal situation. The distinction between two faults brings up the issue of fault isolation of the actual fault and an assumed fault.

The distinction between partial reconstruction and complete reconstruction is highlighted. However, these two cases can be unified using singular-value decomposition and the Moore–Penrose pseudoinverse, which makes complete reconstruction a special case for partial reconstruction. Similarly, complete isolatability is also made a special case for partial isolatability.

The conditions described in the article are applied to a simulated separation process. The results show the importance of understanding and using the properties of detectability, reconstructability, and isolatability in process fault diagnosis. These properties are easy to visualize and apply using the notion of fault subspaces. Finally, the unreconstructed variance was also used in the simulated process to determine the optimal number of principal components and the dimension of the fault subspaces for best reconstruction.

The conditions derived in the article use the SPE to detect faults. It should be noted that the T^2-test has also been used in the literature to detect faults that cause a significant shift in the PCS. While the SPE-based results apply to most situations, they do not cover faults that increase the T^2 index but do not affect SPE. These types of faults are consistent with the model correlation structure, have similar behavior to normal throughput changes, and are considered not detectable based on SPE detectability. However, use of the T^2 index can in fact detect such faults, provided a distinction between these types of faults and normal throughput changes is made. The detectability, reconstructability, and isolatability conditions using both SPE and T^2 indices deserve further study.

Another issue of importance is the existence of dynamic transients in the data. In this case, the principal components are correlated in time. Although some form of low-pass filtering can reduce the effect of dynamic transients, a complete solution sould be to use dynamic PCA, which removes time-correlation in the PCS. Extension of the conditions derived in this article to the dynamic situation will be studied in the future.

Acknowledgment

Financial support from ALCOA Foundation, Dupont, and Fisher-Rosemount Systems, Inc., for this research is gratefully acknowledged.

Notation

a, b = scalars
$\boldsymbol{a}$, $\boldsymbol{b}$ = vectors
$\mathcal{E}\{\cdot\}$ = expectation
l_i = dimension of the ith fault subspace
m = number of sensors
$\mathfrak{N}$ = null space
$\mathfrak{R}$ = range space
$\Re$ = real
$\boldsymbol{x}_j$ = reconstructed sample vector when $\mathcal{F}_j$ is assumed

Superscripts and subscripts

$^{\circ}$ = normalized matrix
$^{\perp}$ = perpendicular
$\bar{}$ = average
* = uncorrupted portion
$^{+}$ = Moore-Penrose pseudo-inverse
^{T} = transpose

Literature Cited

Albert, A., *Regression and the Moore-Penrose Pseudoinverse*, Academic Press, New York (1972).

De Veaux, R. D., L. H. Ungar, and J. M. Vinson, "Statistical Approaches to Fault Analysis in Multivariate Process Control," *Proc. Amer. Control Conf.*, Seattle, WA, p. 1274 (1995).

Dunia, R., J. Qin, T. F. Edgar, and T. J. McAvoy, "Identification of Faulty Sensors using Principal Component Analysis," *AIChE J.*, **42**, 2797 (1996a).
Dunia, R., J. Qin, T. F. Edgar, and T. J. McAvoy, "Sensor Fault Identification and Reconstruction using Principal Component Analysis," *Proc. IFAC Cong.* vol. N, International Federation of Automatic Control, San Francisco, p. 259 (1996b).
Dunia, R., J. Qin, T. F. Edgar, and T. J. McAvoy, "Use of Principal Component Analysis for Sensor Fault Identification," *Comput. Chem. Eng.*, **20**, 713 (1996c).
Dunia, R., and S. J. Qin, "A Unified Geometric Approach to Process and Sensor Fault Identification and Reconstruction: The Unidimensional Fault Case," *Comput. Chem. Eng.*, in press (1998).
Jackson, J. E., "Principal Component and Factor Analysis: I. Principal Components," *J. Qual. Technol.*, **12**, 201 (1980).
Jackson, J. E., *A User's Guide to Principal Components*, Wiley-Interscience, New York (1991).
Jackson, J. E., and G. S. Mudholkar, "Control Procedures for Residuals Associated with Principal Component Analysis," *Technometrics*, **21**, 341 (1979).
Keller, J. Y., M. Darouach, and G. Krzakala, "Fault Detection of Multiple Biases Process Leaks in Linear Steady State Systems," *Comput. Chem. Eng.*, **18**, 1001 (1994).
Kourti, T., and J. F. MacGregor, "Multivariable SPC Methods for Monitoring and Diagnosing of Process Performance," *Proc. PSE*, p. 739 (1994).
Kresta, J., J. F. MacGregor, and T. E. Marlin, "Multivariable Statistical Monitoring of Process Operating Performance," *Can. J. Chem. Eng.*, **69**, 35 (1991).
Krzanowski, W. J., "Between-Groups Comparison of Principal Components," *J. Amer. Stat. Assoc.*, **74**, 703 (1979).
Ku, W., R. Storer, and C. Georgakis, "Disturbance Detection and Isolation by Dynamic Principal Component Analysis," *Chemometrics Intelligent Lab. Syst.*, **30** 179 (1995).
MacGregor, J. F., and T. Kourti, "Statistical Process Control of Multivariable Processes," *Control Eng. Practice* **3**, 403 (1995).
MacGregor, J. F., P. Nomikos, and T. Kourti, "Multivariable Statistical Process Control of Batch Processes using PCA and PLS," *Proc. IFAC ADCHEM Symp.*, Japan, p. 525 (1994).
McBrayer, K. F., *Detection and Identification of Bias in Nonlinear Dynamic Processes*, PhD Thesis, Dept. of Chemical Engineering, Univ. of Texas at Austin (1995).
Miller, P., R. Swanson, and C. Heckler, "Contribution Plots: The Missing Link in Multivariate Quality Control," *Conf. ASQC and ASA*, Milwaukee, WI (1993).
Ogata, K., *Discrete Time Control Systems*, Prentice Hall, Englewood Cliffs, NJ (1987).
Raich, A. C., and A. Cinar, "Multivariable Statistical Methods for Monitoring Continuous Processes: Assessment of Discrimination Power of Disturbance Models and Diagnosis of Multiple Disturbances," *Proc. InCINC'94* (1994).
Strang, G., *Linear Algebra and Its Applications*, Academic Press, New York (1980).
Tong, H., and C. M. Crowe, "Detection of Gross Errors in Data Reconciliation by Principal Component Analysis," *AIChE J.*, **41**, 1712 (1995).
Wise, B. M., and N. L. Ricker, "Recent Advances in Multivariate Statistical Process Control: Improving Robustness and Sensitivity," *Proc. IFAC ADCHEM Symp.*, p. 125, France (1991).
Wold, S., K. Esbensen, and P. Geladi, "Principal Component Analysis," *Chemometrics Intelligent Lab. Syst.*, **2**, 37 (1987).

Appendix A

Substituting the SVD form of Eq. 10 into Eq. 21 leads to

$$f_i = \arg\min \| \tilde{x} - \tilde{\Xi}_i^{\circ} \tilde{D}_i \tilde{V}_i^T f_i \|^2.$$

Solving for $\tilde{V}_i^T f_i$, we obtain

$$\tilde{V}_i^T f_i = \tilde{D}_i^{-1} \tilde{\Xi}_i^{\circ T} \tilde{x}.$$

As a consequence, a complete solution of f_i is

$$f_i = \tilde{V}_i \tilde{D}_i^{-1} \tilde{\Xi}_i^{\circ T} \tilde{x} + \tilde{V}_i^{\perp} b,$$

where $b \in \Re^{l_i - \tilde{l}_i}$ represents an arbitrary displacement in the vanishing or unreconstructable directions. The first term on the righthand side represents the reconstruction in the nonvanishing directions. The *partial reconstruction* is defined as the reconstruction in the nonvanishing directions only, which sets $b = 0$:

$$f_i = \tilde{V}_i \tilde{D}_i^{-1} \tilde{\Xi}_i^{\circ T} \tilde{x} = \tilde{\Xi}_i^{+} \tilde{x} = \tilde{\Xi}_i^{+} \tilde{C} x,$$

where $\tilde{\Xi}_i^{+}$ is the Moore–Penrose pseudoinverse given in Eq. 26. Now we only need to show that

$$\tilde{\Xi}_i^{+} \tilde{C} = \tilde{\Xi}_i^{+}$$

to complete the proof of Eq. 25. From the properties of the Moore–Penrose pseudoinverse (Albert, 1972), $\tilde{\Xi}_i^{+}$ is the pseudoinverse of $\tilde{\Xi}_i$ if and only if:

(1) $\tilde{\Xi}_i \tilde{\Xi}_i^{+}$ and $\tilde{\Xi}_i^{+} \tilde{\Xi}_i$ are symmetric.
(2) $\tilde{\Xi}_i^{+} \tilde{\Xi}_i \tilde{\Xi}_i^{+} = \tilde{\Xi}_i^{+}$.
(3) $\tilde{\Xi}_i \tilde{\Xi}_i^{+} \tilde{\Xi}_i = \tilde{\Xi}_i$.

To show that $\tilde{\Xi}_i^{+} \tilde{C} = \tilde{\Xi}_i^{+}$, we need only to show that:

(i) $\tilde{\Xi}_i (\tilde{\Xi}_i^{+} \tilde{C})$ and $(\tilde{\Xi}_i^{+} \tilde{C}) \tilde{\Xi}_i$ are symmetric.
(ii) $(\tilde{\Xi}_i^{+} \tilde{C}) \tilde{\Xi}_i (\tilde{\Xi}_i^{+} \tilde{C}) = (\tilde{\Xi}_i^{+} \tilde{C})$.
(iii) $\tilde{\Xi}_i (\tilde{\Xi}_i^{+} \tilde{C}) \tilde{\Xi}_i = \tilde{\Xi}_i$.

Item (i) is easily shown by using the fact that $\tilde{C}$ is symmetric and $\tilde{C} \tilde{\Xi}_i = \tilde{\Xi}_i$. Item (ii) is shown as follows:

$$\left(\tilde{\Xi}_i^{+} \tilde{C}\right) \tilde{\Xi}_i \left(\tilde{\Xi}_i^{+} \tilde{C}\right) = \left(\tilde{\Xi}_i^{+} \tilde{\Xi}_i \tilde{\Xi}_i^{+}\right) \tilde{C} = \left(\tilde{\Xi}_i^{+} \tilde{C}\right).$$

Similarly, item (iii) is easily shown using $\tilde{C} \tilde{\Xi}_i = \tilde{\Xi}_i$.

Appendix B

The inequality constraint $\| \tilde{x}^* \| \le \delta$ is added to the objective function in Eq. 63, leading to the following optimization problem:

$$\min_{x^*} \Phi \tag{B1}$$

where

$$\Phi = \mathrm{SPE}_{j|i} + \mu (x^{*T} x^* + \varphi^2 - \delta^2) \tag{B2}$$

$$= \| \left(I - \tilde{\Xi}_j^{\circ} \tilde{\Xi}_j^{\circ T} \right) \left(\tilde{x}^* + \tilde{\Xi}_i^{\circ} \tilde{f} \right) \|^2 + \mu (x^{*T} x^* + \varphi^2 - \delta^2). \tag{B3}$$

The variables μ and φ represent the Lagrange multiplier and the slack variable of the inequality constraint, respectively. Because the eigenvalues of $I - \tilde{\Xi}_j^{\circ} \tilde{\Xi}_j^{\circ T}$ are zeros or ones, a global minimum is expected from Eq. (B1). To calculate such a minimum, two possible cases need to be considered.

1. $\mu = 0$, in which case the inequality constraint is not active. If $\tilde{x}^*$ can be freely chosen to minimize the $SPE_{j|i}$, the minimum is obtained when $\tilde{x}^* + \tilde{\Xi}_i^\circ \tilde{f} \in \Re\{\tilde{\Xi}_j^\circ\}$, in which case $SPE_{j|i} = 0$. This case should be avoided because $SPE_{j|i} = 0 \leq \delta^2$ and no sufficient condition for isolatability is achieved. A way to eliminate this situation is by increasing the magnitude of $\tilde{f}$ until the constraint is active and $\tilde{x}^* + \tilde{\Xi}_i^\circ \tilde{f} = \tilde{\Xi}_j^\circ \gamma \in \Re\{\tilde{\Xi}_j^\circ\}$ is infeasible. Therefore, we would like to find a condition for $\tilde{f}$ such that

$$\| \tilde{x}^* \|^2 = \| \tilde{\Xi}_j^\circ \gamma - \tilde{\Xi}_i^\circ \tilde{f} \|^2 > \delta^2 \tag{B4}$$

The preceding expression should be satisfied for any $\gamma \in \Re^{\tilde{l}_j}$, particularly for

$$\min_\gamma \| \tilde{\Xi}_j^\circ \gamma - \tilde{\Xi}_i^\circ \tilde{f} \|^2, \tag{B5}$$

which provides the worst case for Eq. B4. Note that

$$\| \tilde{\Xi}_j^\circ \gamma - \tilde{\Xi}_i^\circ \tilde{f} \|^2 = \gamma^T \gamma - 2\gamma^T \tilde{\Xi}_j^{\circ T} \tilde{\Xi}_i^\circ \tilde{f} + \tilde{f}^T \tilde{f}$$

has a minimum at $\gamma = \tilde{\Xi}_j^{\circ T} \tilde{\Xi}_i^\circ \tilde{f}$. Substitution in Eq. B4 gives

$$\| \left(I - \tilde{\Xi}_j^{\circ T} \tilde{\Xi}_j^\circ \right) \tilde{\Xi}_j^\circ \tilde{f} \| > \delta. \tag{B6}$$

This condition assures that there is no γ such that $SPE_{j|i} = 0$.

2. $\varphi = 0$, in which case the constraint is active. The differentiation of the objective function in Eq. B1 with respect to $\tilde{x}^*$ and φ leads to the following set of equations:

$$\left(I - \tilde{\Xi}_j^\circ \tilde{\Xi}_j^{\circ T} \right) \left(\tilde{x}^* + \tilde{\Xi}_i^\circ \tilde{f} \right) + \mu \tilde{x}^* = \mathbf{0}$$

$$x^{*T} x^* - \delta^2 = 0.$$

Solving for $\tilde{x}^*$ in the first equation, we obtain

$$\tilde{x}^* = -\left[\left((1-\mu) I - \tilde{\Xi}_j^\circ \tilde{\Xi}_j^{\circ T} \right) \right]^{-1} \left(I - \tilde{\Xi}_j^\circ \tilde{\Xi}_j^{\circ T} \right) \tilde{\Xi}_i^\circ \tilde{f}.$$

The matrix inversion lemma (Ogata, 1987) is used to obtain the following relation:

$$\left[(1+\mu) I - \tilde{\Xi}_j^\circ \tilde{\Xi}_j^{\circ T} \right]^{-1} = -\left[\frac{1}{1+\mu} I + \frac{1}{(1+\mu)\mu} \tilde{\Xi}_j^\circ \tilde{\Xi}_j^{\circ T} \right],$$

which leads to

$$\tilde{x}^* = -\frac{1}{\mu} \left(I - \tilde{\Xi}_j^\circ \tilde{\Xi}_j^{\circ T} \right) \tilde{\Xi}_i^\circ \tilde{f}$$

and because $\| \tilde{x}^* \| = \delta$, we have

$$\tilde{x}^* = \frac{\pm \delta \left(I - \tilde{\Xi}_i^\circ \tilde{\Xi}_j^{\circ T} \right) \tilde{\Xi}_i^\circ \tilde{f}}{\| \left(I - \tilde{\Xi}_j^\circ \tilde{\Xi}_j^{\circ T} \right) \tilde{\Xi}_i \tilde{f} \|}. \tag{B7}$$

Note that this solution makes $\tilde{x}^* \in \tilde{\mathcal{S}}_j^\perp$. Substitution of $\tilde{x}^*$ in Eq. 61 provides a sufficient condition for fault identifiability for the worst possible $\tilde{x}^*$ when the constraint is active,

$$\| \left(I - \tilde{\Xi}_j^\circ \tilde{\Xi}_j^{\circ T} \right) \tilde{\Xi}_i^\circ \tilde{f} \| > 2\delta. \tag{B8}$$

Such a condition assures that $\mathcal{F}_i$ is isolated from $\mathcal{F}_j$ when the constraint is active. Note that the preceding inequality is also a sufficient condition to avoid case 1. Therefore, Eq. B8 provides the sufficient condition for fault isolation when $\mathcal{F}_i$ and $\mathcal{F}_j$ are partially reconstructed.

Appendix C

To illustrate the description of a process fault we first consider $\mathcal{F}_{13}$, which corresponds to a leak at the second column reboiler. The right side of Figure C1 shows a detail of the leak that affects sensors 8 to 10. An amount a of fluid leaving from the leak causes sensors 8 and 9 to be affected by the same amount. Because the flow is ramified downstream of sensor 9, however, a portion of a denoted by b affects sensor 10. Therefore, $\mathcal{S}_{13}$ can be characterized by the followed vector:

$$\Xi_{13} f = [0 \;\; 0 \;\; 0 \;\; 0 \;\; 0 \;\; 0 \;\; 0 \;\; -a \;\; -a \;\; -b \;\; 0 \;\; 0]^T$$

$$= \begin{bmatrix} 0 & 0 & 0 & 0 & 0 & 0 & 0 & 1 & 1 & 0 & 0 & 0 \\ 0 & 0 & 0 & 0 & 0 & 0 & 0 & 0 & 0 & 1 & 0 & 0 \end{bmatrix}^T \begin{bmatrix} -a \\ -b \end{bmatrix}.$$

To make the fault directions orthonormal we choose

$$\Xi_{13} = \begin{bmatrix} 0 & 0 & 0 & 0 & 0 & 0 & 0 & \sqrt{2}/2 & \sqrt{2}/2 & 0 & 0 & 0 \\ 0 & 0 & 0 & 0 & 0 & 0 & 0 & 0 & 0 & 1 & 0 & 0 \end{bmatrix}^T.$$

Therefore, Ξ_{13} describes any displacement on $\mathcal{S}_{13}$, that is, any possible leak at the second reboiler.

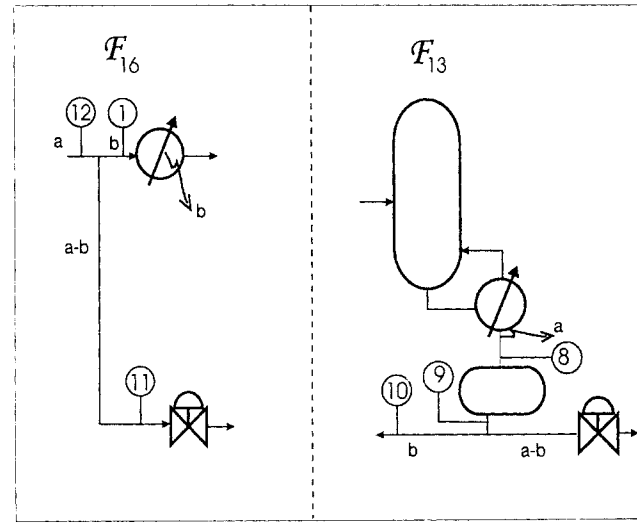

Figure C1. Description of $\mathcal{F}_{13}$ and $\mathcal{F}_{16}$ for the loss of material at the locations indicated by such faults in Figure 10.

In the case of a fault close to the feed stream, like $\mathfrak{F}_{16}$, the fault will cause the total feed to increase and the split ratio between the two branches to change. We assume that an incremental amount, a, coming into the feed is distributed in b and $a-b$ between sensors 1 and 11, respectively. As the left side of Figure C1 illustrates, the amount b goes through the leak. Therefore,

$$\Xi_{16} f = [b \quad 0 \quad 0 \quad 0 \quad 0 \quad 0 \quad 0 \quad 0 \quad 0 \quad 0 \quad a-b \quad a]^T$$

$$= \begin{bmatrix} 0 & 0 & 0 & 0 & 0 & 0 & 0 & 0 & 0 & 0 & 1 & 1 \\ 1 & 0 & 0 & 0 & 0 & 0 & 0 & 0 & 0 & 0 & -1 & 0 \end{bmatrix}^T \begin{bmatrix} a \\ b \end{bmatrix}.$$

The orthonormal fault direction Ξ_{16} is provided by SVD,

$$\Xi_{16} = \begin{bmatrix} -\sqrt{6}/6 & 0 & 0 & 0 & 0 & 0 & 0 & 0 & 0 & 0 & \sqrt{6}/3 & \sqrt{6}/6 \\ -\sqrt{2}/2 & 0 & 0 & 0 & 0 & 0 & 0 & 0 & 0 & 0 & 0 & -\sqrt{2}/2 \end{bmatrix}^T.$$

Faults $\mathfrak{F}_{14}$ and $\mathfrak{F}_{15}$ can be represented from the feed side (like $\mathfrak{F}_{16}$) or product side (like $\mathfrak{F}_{13}$), depending on which side provides the subspace with less dimension and with more reliable sensors. Like the preceding derivation, the fault directions for faults $\mathfrak{F}_{14}$ and $\mathfrak{F}_{15}$ are

$$\Xi_{14} = \begin{bmatrix} 0 & 0 & 0 & 0 & 0 & 1 & 1 & 0 & 0 & 0 & 0 & 0 \\ 0 & 0 & 0 & 0 & 0 & 0 & -1 & 1 & 1 & 1 & 0 & 0 \\ 0 & 0 & 0 & 0 & 0 & 0 & 0 & 0 & 0 & -1 & 0 & 0 \end{bmatrix}^T$$

$$\text{After SVD} \rightarrow \begin{bmatrix} 0 & 0 & 0 & 0 & 0 & 0.1585 & 0.5788 & -0.4203 & -0.4203 & -0.5354 & 0 & 0 \\ 0 & 0 & 0 & 0 & 0 & -0.6899 & -0.5009 & -0.1889 & -0.1889 & -0.4492 & 0 & 0 \\ 0 & 0 & 0 & 0 & 0 & 0.3146 & -0.1187 & 0.4332 & 0.4332 & -0.7153 & 0 & 0 \end{bmatrix}^T$$

and

$$\Xi_{15} = \begin{bmatrix} 0 & 0 & 0 & 0 & 0 & 0 & 0 & 0 & 0 & 0 & 1 & 1 \\ 1 & 1 & 1 & 1 & 0 & 0 & 0 & 0 & 0 & 0 & -1 & 0 \\ 0 & 0 & -1 & -1 & 0 & 0 & 0 & 0 & 0 & 0 & 0 & 0 \end{bmatrix}^T$$

$$\text{After SVD} \rightarrow \begin{bmatrix} -0.3546 & -0.3546 & -0.5237 & -0.5237 & 0 & 0 & 0 & 0 & 0 & 0 & 0.4391 & 0.0846 \\ 0 & 0 & -0.3162 & -0.3162 & 0 & 0 & 0 & 0 & 0 & 0 & -0.6325 & -0.6325 \\ 0.5237 & 0.5237 & -0.3546 & -0.3546 & 0 & 0 & 0 & 0 & 0 & 0 & -0.0846 & 0.4391 \end{bmatrix}^T.$$

Manuscript received Jan 21, 1997, and revision received Apr. 20, 1998.